Electronic Supplementary Information

Oxatub[4]arene: A Molecular "Transformer" Capable of Hosting a Wide Range of Organic Cations

Fei Jia, Hao-Yi Wang, Dong-Hao Li, Liu-Pan Yang and Wei Jiang*
Department of Chemistry, South University of Science and Technology of China, Xueyuan Blvd 1088, Nanshan District, Shenzhen, 518055, P. R. China
**E-mail: jiangw@sustc.edu.cn*

Table of Contents

1. Experimental Section

1.1 General. All the reagents involved in this research were commercially available and used without further purification unless otherwise noted. Solvents were either employed as purchased or dried prior to use by standard laboratory procedures. ^{1}H NMR, and ^{1}H-^{1}H ROESY NMR spectra were recorded on Bruker Avance-400 or 600 spectrometers. All chemical shifts are reported in *ppm* with residual solvents or TMS (tetramethylsilane) as the internal standards. Electrospray-ionization time-of-flight high-resolution mass spectrometry (ESI-TOF-HRMS) experiments were conducted on an applied Q EXACTIVE mass spectrometry system. Molecular simulations were performed at the Semi-Empirical PM6 level of theory by using Spartan'14 (Wavefunction, Inc.). The synthesis of Oxatub[4]arene (**TA4**) has been reported.[1]

1.2 Isothermal titration calorimetry, ITC. Titration experiments were carried out in 1,2-dichloroethane/CH_3CN 1 : 1 (v/v) at 25 °C on a Nano ITC LV – 190 μL (Waters GmbH, TA Instruments, Eschborn, Germany). In a typical experiment, a 190 μL solution of **TA4** was placed in the sample cell at a concentration of 0.16 mM, and 50 μL of a solution of the hexafluorophosphate salt (1.0 mM in the same solvent) was in the injection syringe. The titrations consisted of 25 consecutive injections of 1.96 μL each with a 5 min interval between injections. Heats of dilution, measured by titration of the salt into the sample cell with blank solvent, were subtracted from each data set. All solutions were degassed prior to titration. The data were analysed using the instrumental internal software package and fitted with a 1:1 binding model. Errors are smaller than ±10%.

---

1 F. Jia, Z. He, L.-P. Yang, Z.-S. Pan, M. Yi, R.-W. Jiang and W. Jiang. *Chem. Sci.*, 2015, ***6***, 6731-6738.

2. ^{1}H NMR spectra of the Complexes

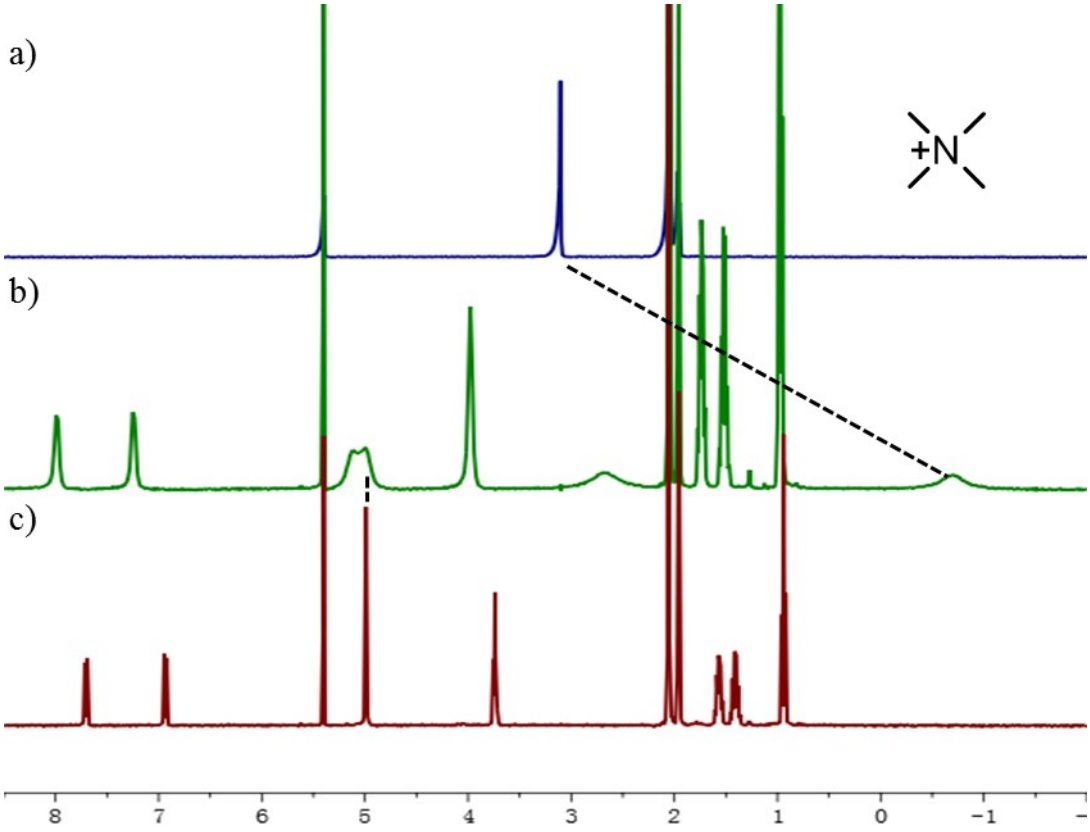

Fig. S1 ^{1}H NMR spectra (400 MHz, CD_2Cl_2:CD_3CN=1:1, 2.0 mM, 298 K) of (a) Guest **1-PF$_6$**, (c) **TA4** and (b) their equimolar mixture. In the host-guest mixture, the protons of the guest shifted upfield, while the protons of **TA4** becomes slightly broadened and undergo downfield shift, suggesting the formation of the complex between **1-PF$_6$** and **TA4**.

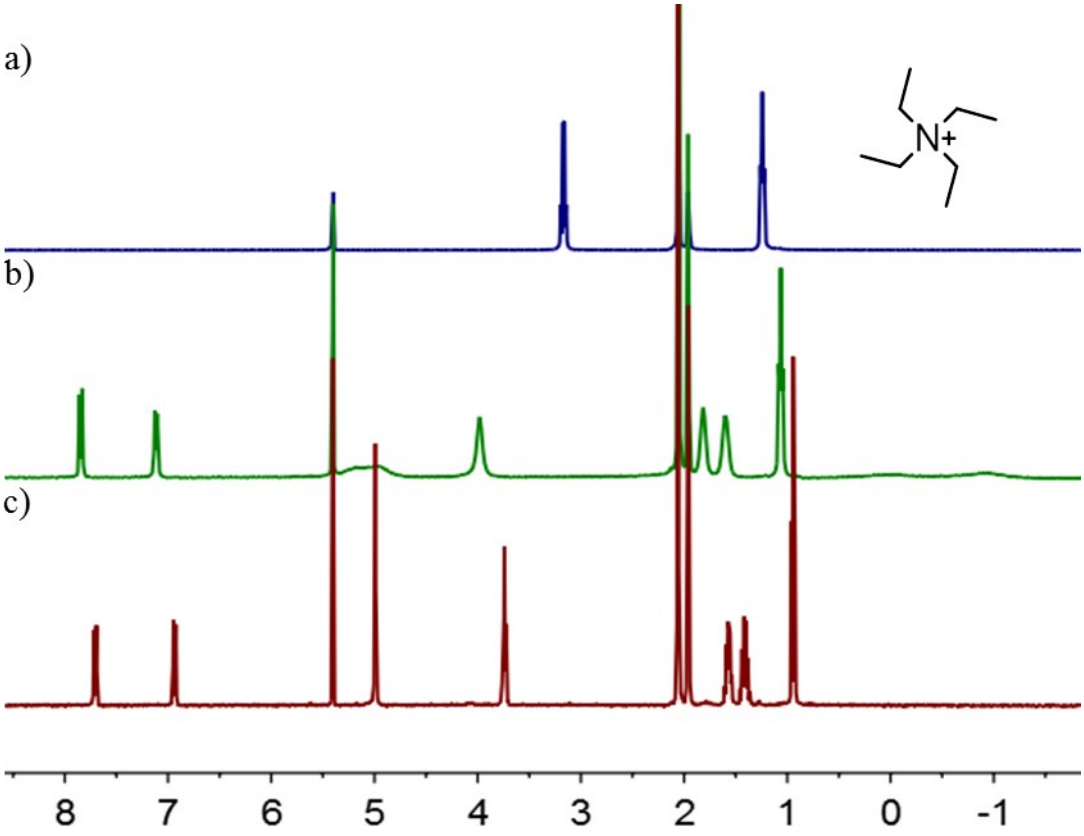

Fig. S2 ^{1}H NMR spectra (400 MHz, CD_2Cl_2:CD_3CN=1:1, 2.0 mM, 298 K) of (a) Guest **2-PF$_6$**, (c) **TA4**, and (b) their equimolar mixture. In the host-guest mixture, the protons of the guest shifted upfield, while the protons of **TA4** becomes broadened and undergo downfield shift, suggesting the formation of the complex between **2-PF$_6$** and **TA4**.

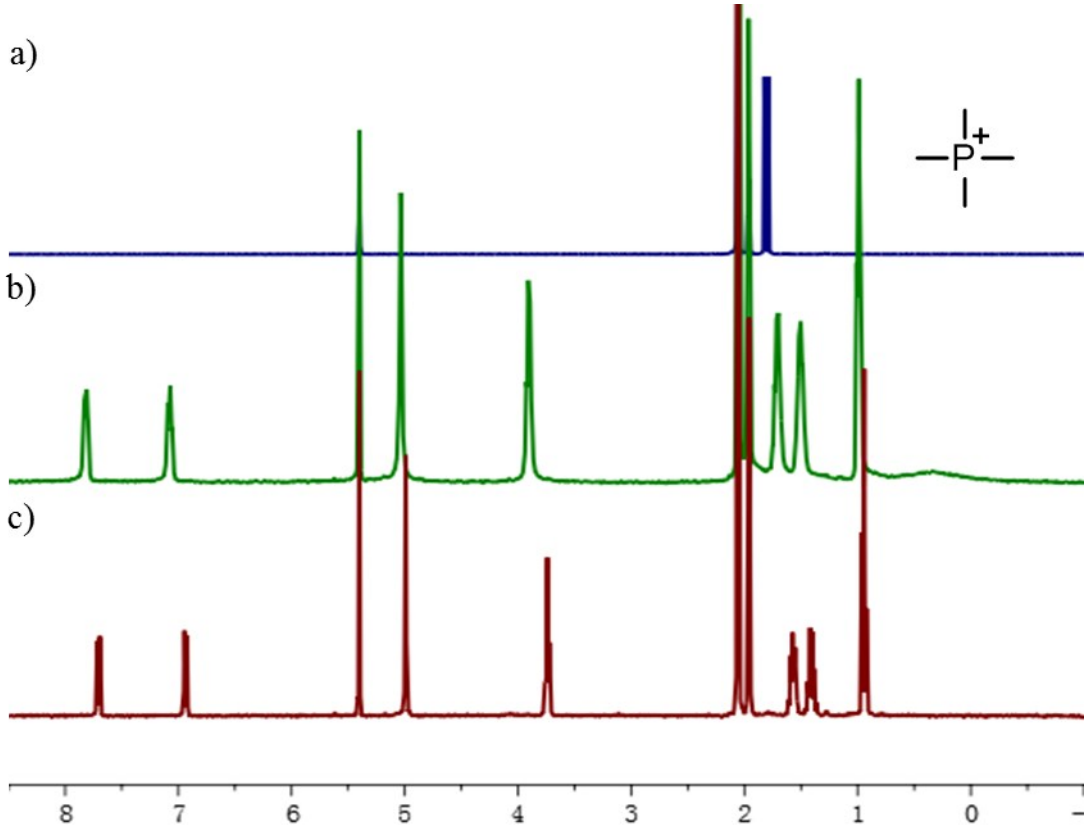

Fig. S3 ^{1}H NMR spectra (400 MHz, CD_2Cl_2:CD_3CN=1:1, 2.0 mM, 298 K) of (a) Guest **3-PF$_6$**, (c) **TA4** and (b) their equimolar mixture. In the host-guest mixture, the protons of the guest became broadened and rolled into the baseline, while the protons of **TA4** shifted downfield, suggesting the complexation between **3-PF$_6$** and **TA4**.

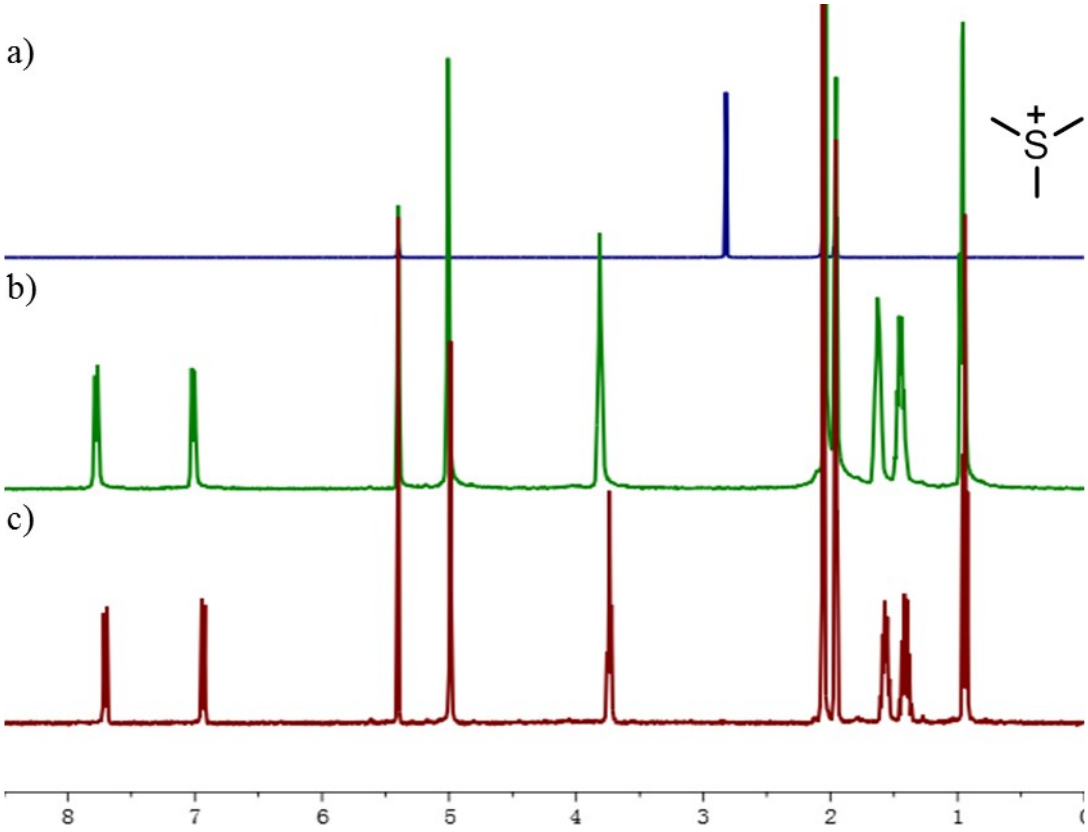

Fig. S4 ^{1}H NMR spectra (400 MHz, CD_2Cl_2:CD_3CN=1:1, 2.0 mM, 298 K) of (a) Guest **4-PF$_6$**, (c) **TA4** and (b) their equimolar mixture. The protons of the guest disappeared into the baseline, while all the protons of **TA4** shifted downfield, suggesting the complexation between **4-PF$_6$** and **TA4**.

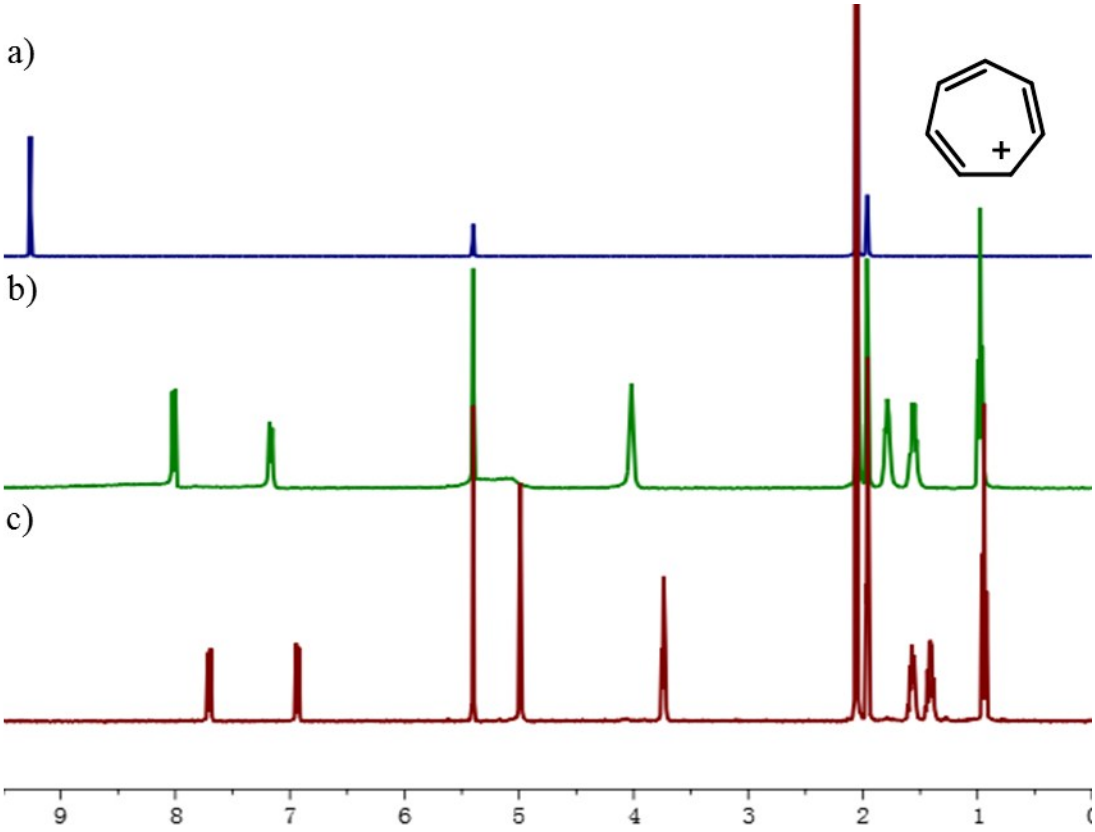

Fig. S5 ^{1}H NMR spectra (400 MHz, CD_2Cl_2:CD_3CN=1:1, 2.0 mM, 298 K) of (a) Guest **5-PF$_6$**, (c) **TA4** and (b) their equimolar mixture. The protons of the guest disappeared into the baseline, while all the protons of **TA4** shifted downfield, indicating the complexation between **5-PF$_6$** and **TA4**.

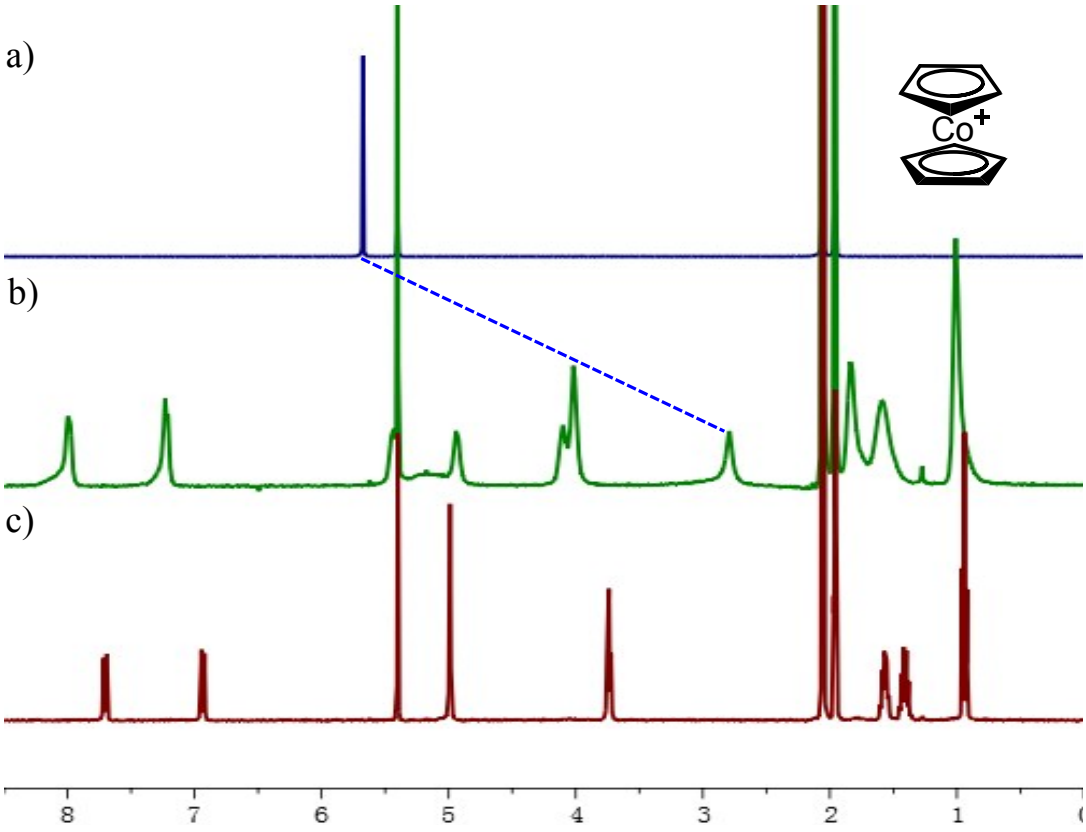

Fig. S6 ^{1}H NMR spectra (400 MHz, CD_2Cl_2:CD_3CN=1:1, 2.0 mM, 298 K) of (a) Guest **6-PF$_6$**, (c) **TA4** and (b) their equimolar mixture. The protons of the guest shifted upfield, while all the protons of **TA4** became broadened and shifted downfield, suggesting the complexation between **6-PF$_6$** and **TA4**.

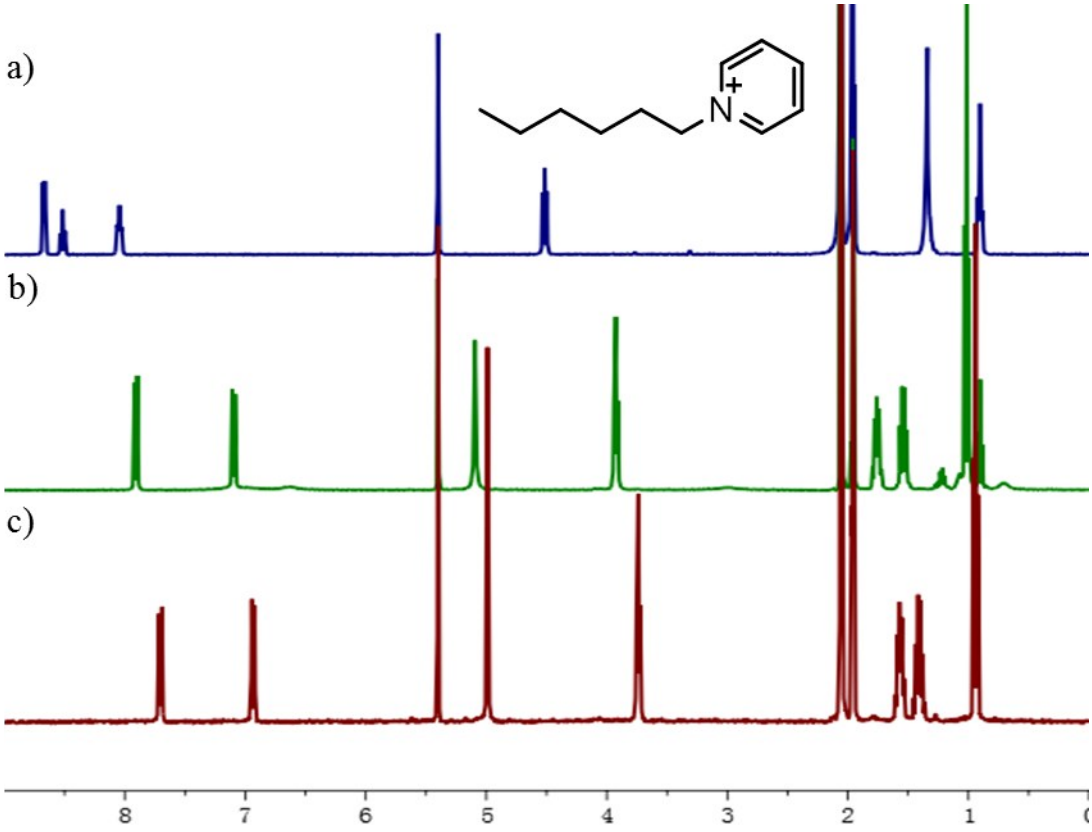

Fig. S7 ^{1}H NMR spectra (400 MHz, CD_2Cl_2:CD_3CN=1:1, 2.0 mM, 298 K) of (a) Guest **7-PF$_6$**, (c) **TA4** and (b) their equimolar mixture. The protons of the guest became significantly broadened and rolled into the baseline, while all the protons of **TA4** shifted downfield, suggesting the complexation between **7-PF$_6$** and **TA4**.

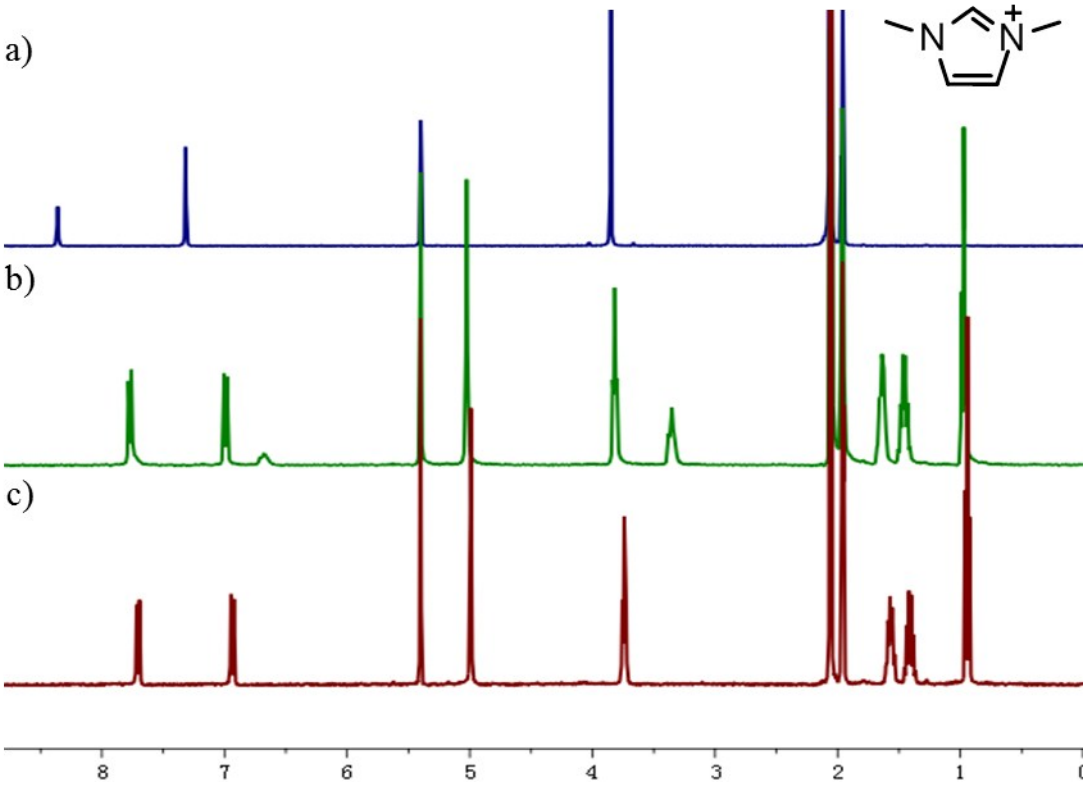

Fig. S8 ^{1}H NMR spectra (400 MHz, CD_2Cl_2:CD_3CN=1:1, 2.0 mM, 298 K) of (a) Guest **8-PF$_6$**, (c) **TA4** and (b) their equimolar mixture. The protons of the guest became significantly broadened and rolled into the baseline, while the protons of **TA4** shifted downfield, suggesting the complexation between **8-PF$_6$** and **TA4**.

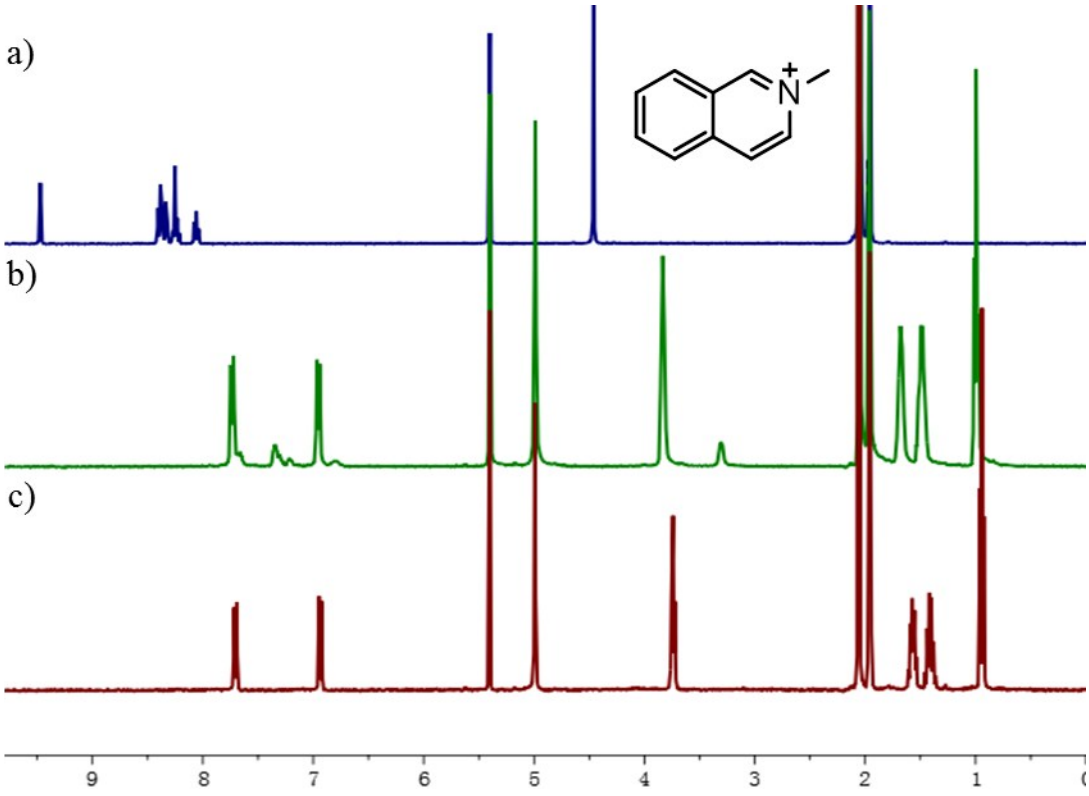

Fig. S9 ^{1}H NMR spectra (400 MHz, CD_2Cl_2:CD_3CN=1:1, 2.0 mM, 298 K) of (a) Guest **9-PF$_6$**, (c) **TA4** and (b) their equimolar mixture. The protons of the guest shifted upfield and became broadened, while the protons of **TA4** shifted downfield, suggesting the complexation between **9-PF$_6$** and **TA4**.

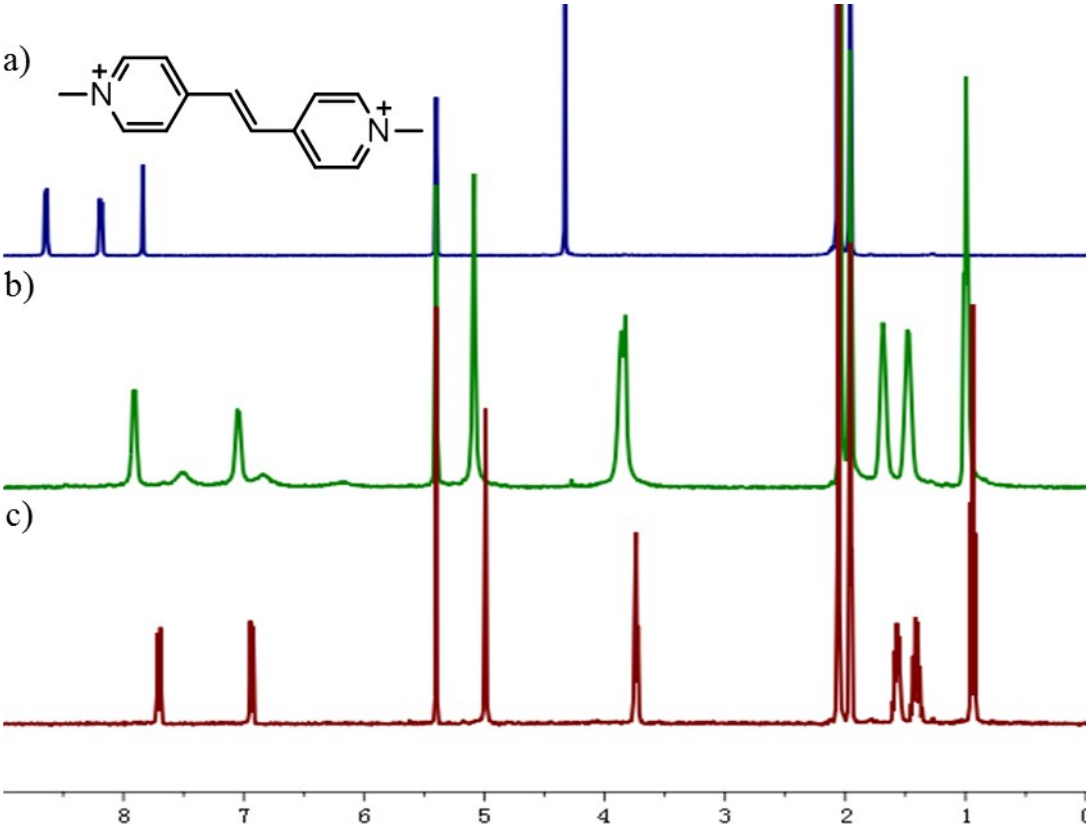

Fig. S10 ^{1}H NMR spectra (400 MHz, CD_2Cl_2:CD_3CN=1:1, 2.0 mM, 298 K) of (a) Guest **10-2PF$_6$**, (c) **TA4** and (b) their equimolar mixture. The protons of guest shifted upfield and became broadened, while all the protons of **TA4** shifted downfield, suggesting the complexation between **10-2PF$_6$** and **TA4**.

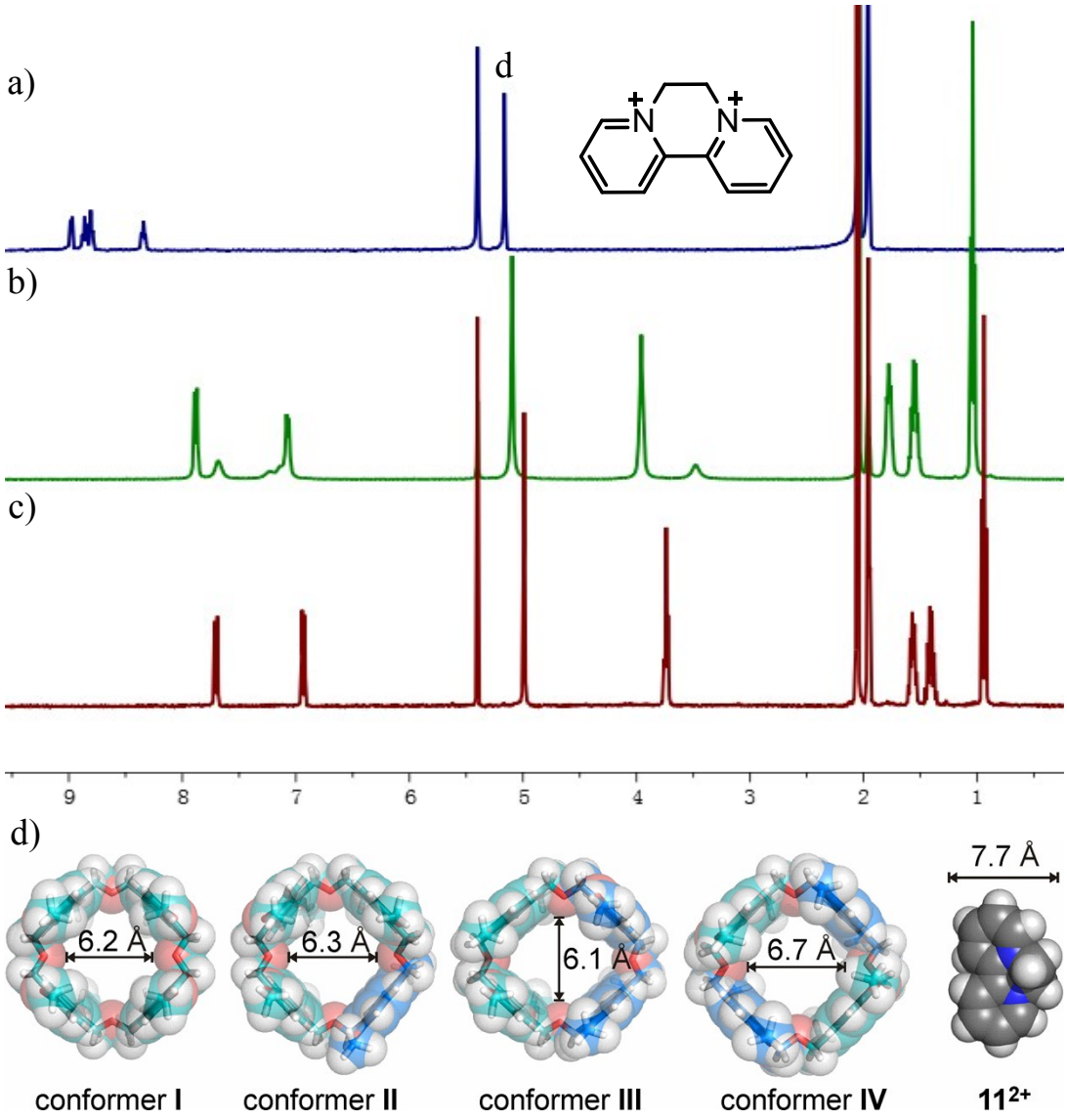

Fig. S11 ^{1}H NMR spectra (400 MHz, CD_2Cl_2:CD_3CN=1:1, 2.0 mM, 298 K) of (a) Guest **11-2PF$_6$**, (c) **TA4** (b) their equimolar mixture. The protons of the guest shifted upfield and became broadened, while all the protons of **TA4** shifted downfield, suggesting the complexation between **11-2PF$_6$** and **TA4**. (d) molecular models to show the cavity size of four conformers and the size of guest **11-2PF$_6$**. In view of the NMR result and molecular model, guest **11-2PF$_6$** may be shallowly encapsulated in the cavity of **TA4**.

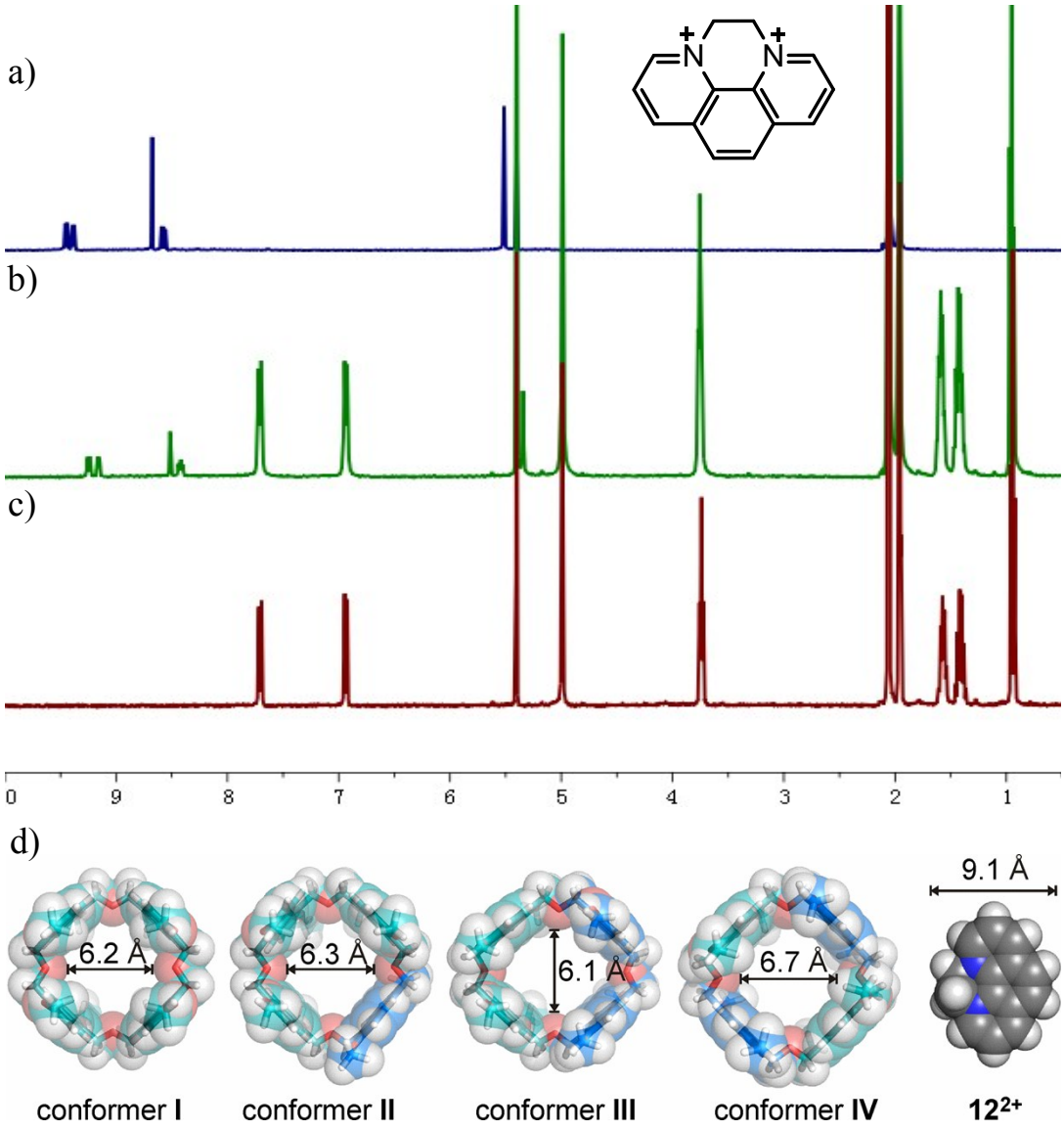

Fig. S12 ^{1}H NMR spectra (400 MHz, CD_2Cl_2:CD_3CN=1:1, 2.0 mM, 298 K) of (a) Guest **12-2PF$_6$**, (c) **TA4** and (b) their equimolar mixture. The protons of the guest shifted upfield, and the protons of **TA4** did not move, suggesting that **TA4** cannot complex with **12-2PF$_6$**. The guest probably sits at the entrance of **TA4**; (d) molecular models to show the cavity size of four conformers and the size of guest **12-2PF$_6$**. Obviously, guest **12-2PF$_6$** is too large to even fit the largest cavity (conformer **IV**). The observed downfield shift of the guests' protons may result from the interactions of **12-2PF$_6$** with the outside surface of **TA4**.

3. Mass spectra of the Complexes

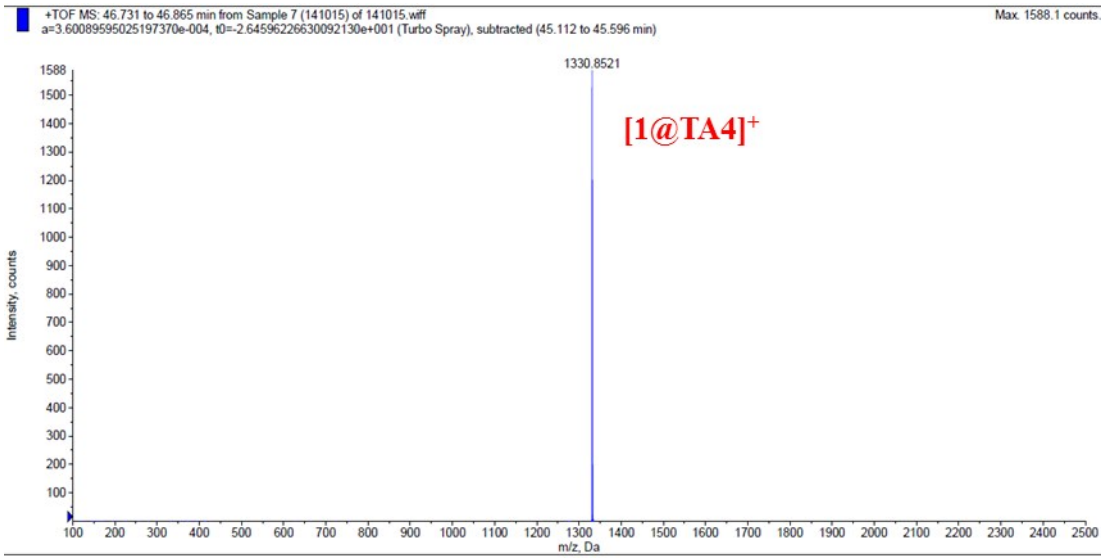

Fig. S13 ESI mass spectrum of **1-PF_6@TA4**. The result indicates **1-PF_6** and **TA4** form a 1:1 complex.

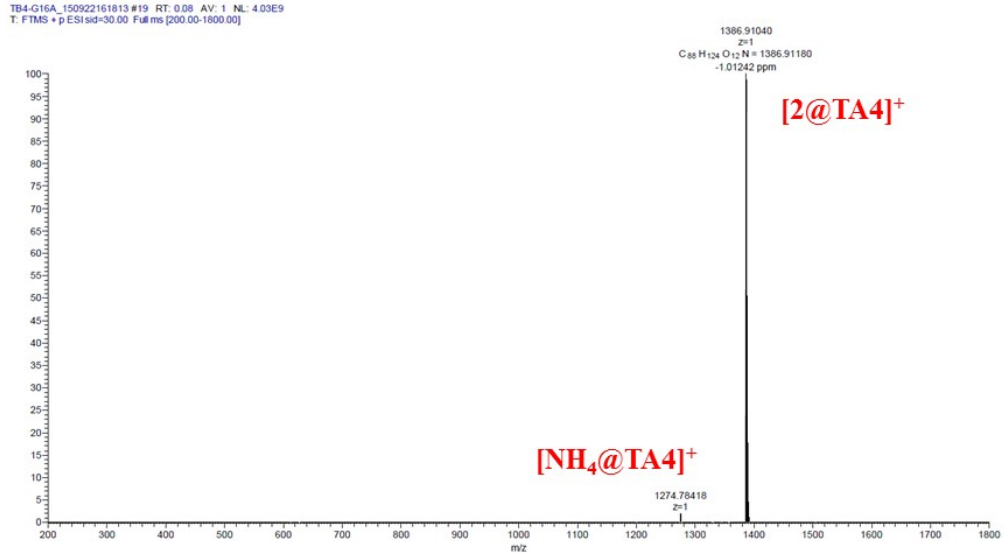

Fig. S14 ESI mass spectrum of **2-PF_6@TA4**. The result indicates **2-PF_6** and **TA4** form a 1:1 complex.

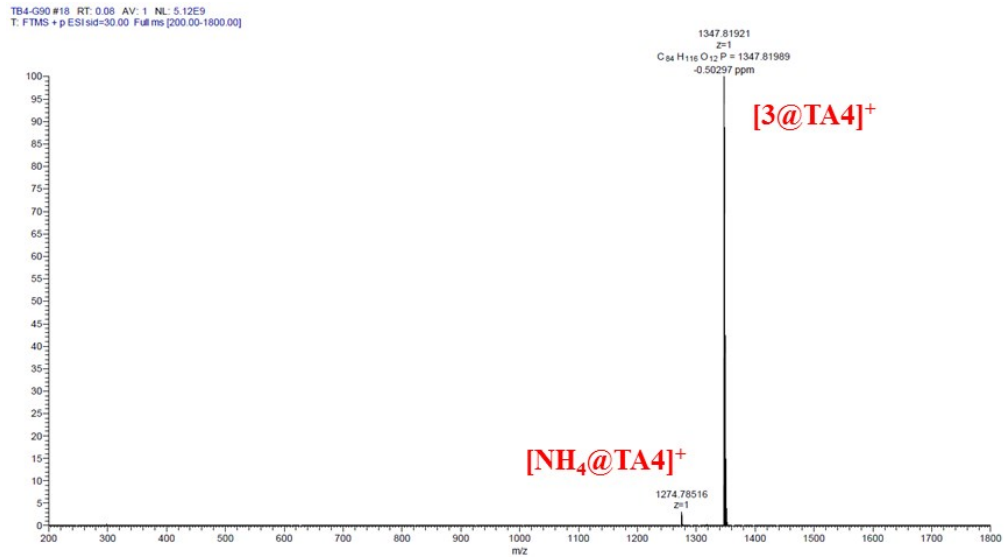

Fig. S15 ESI mass spectrum of **3-PF_6@TA4**. The result indicates **3-PF_6** and **TA4** form a 1:1 complex.

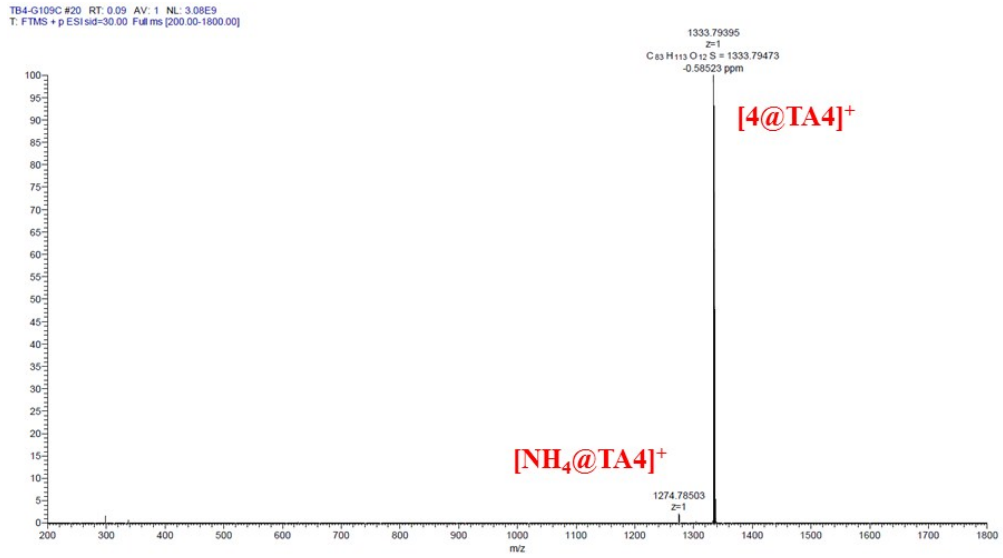

Fig. S16 ESI mass spectrum of **4-PF_6@TA4**. The result indicates **4-PF_6** and **TA4** form a 1:1 complex.

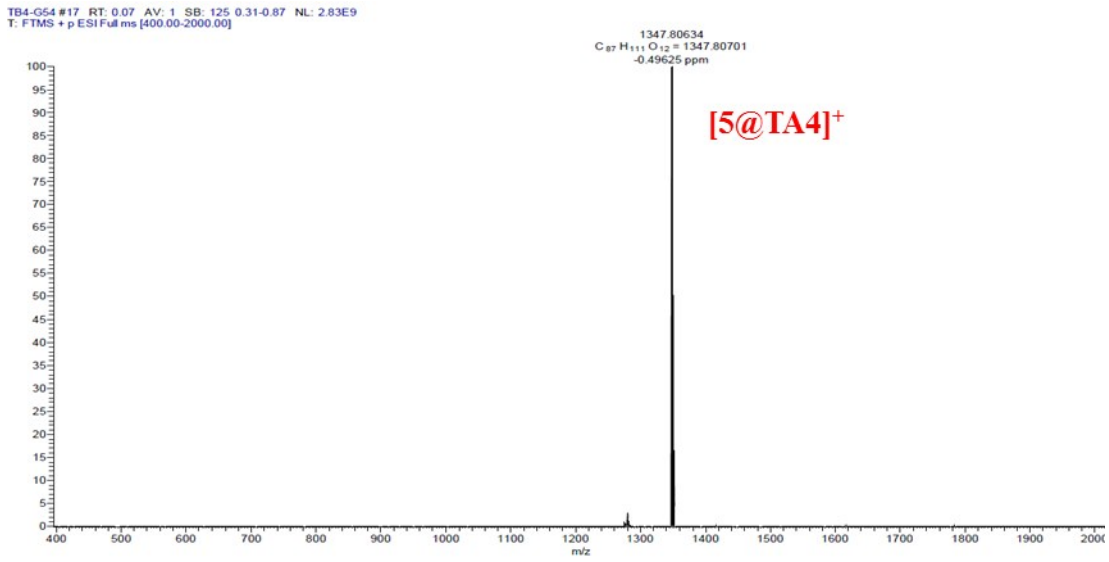

Fig. S17 ESI mass spectrum of **5-PF_6@TA4**. The result indicates**5-PF_6** and **TA4** form a 1:1 complex.

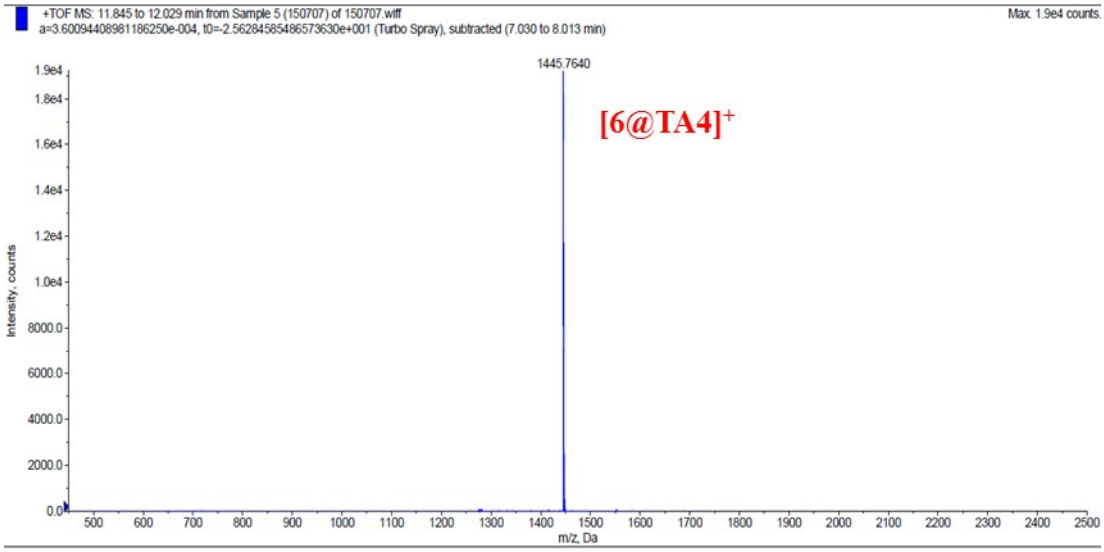

Fig. S18 ESI mass spectrum of **6-PF_6@TA4**. The result indicates **6-PF_6** and **TA4** form a 1:1 complex.

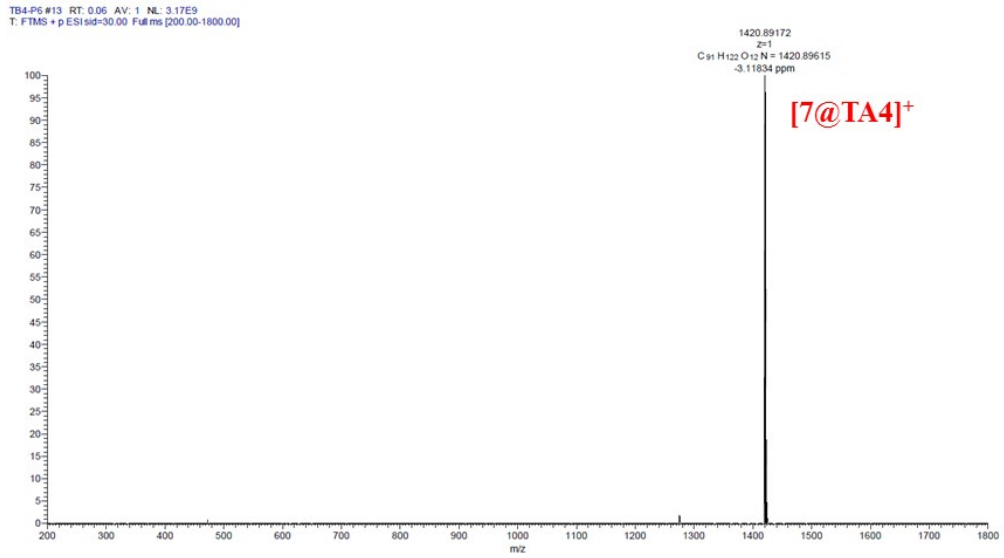

Fig. S19 ESI mass spectrum of **7-PF_6@TA4**. The result indicates **7-PF_6** and **TA4** form a 1:1 complex.

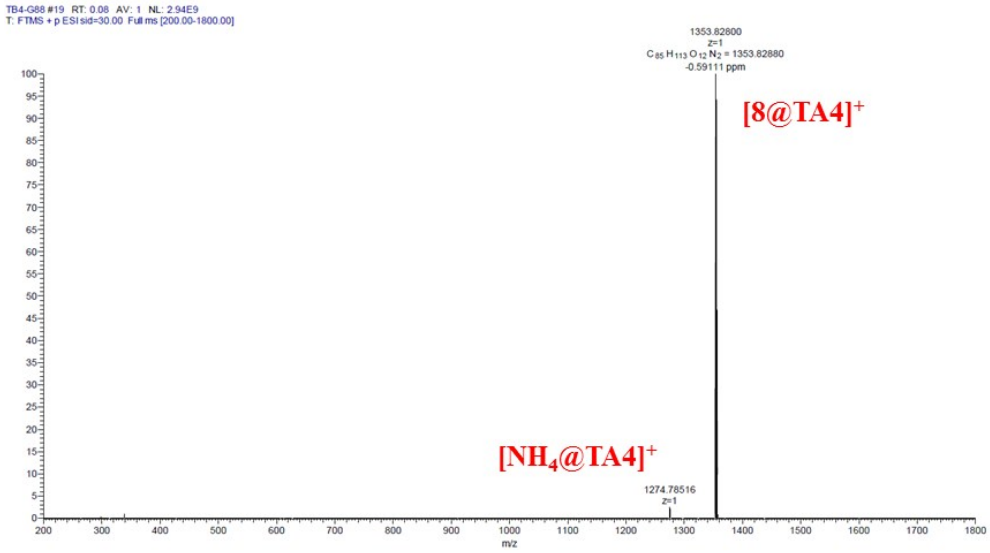

Fig. S20 ESI mass spectrum of **8-PF_6@TA4**. The result indicates **8-PF_6** and **TA4** form a 1:1 complex.

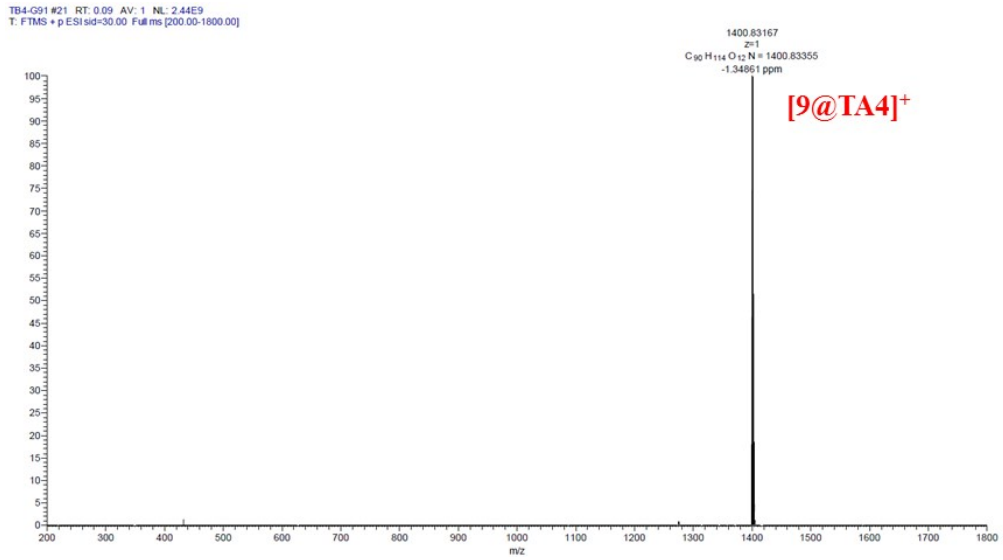

Fig. S21 ESI mass spectrum of **9-PF_6@TA4**. The result indicates **9-PF_6** and **TA4** form a 1:1 complex.

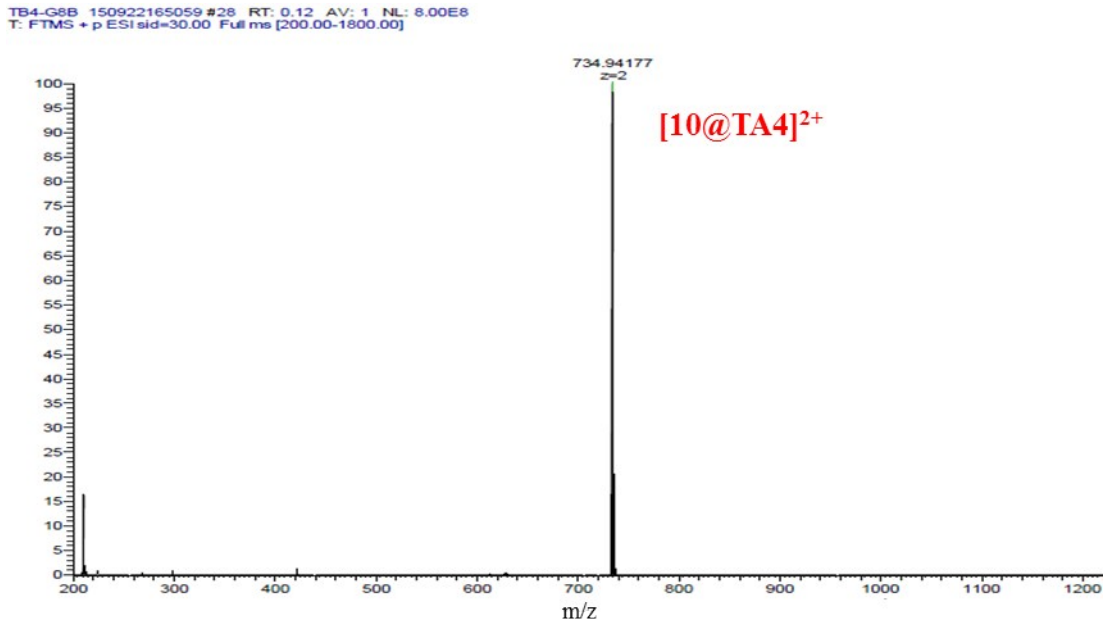

Fig. S22 ESI mass spectrum of **10-2PF_6@TA4**. The result indicates **10-2PF_6** and **TA4** form a 1:1 complex.

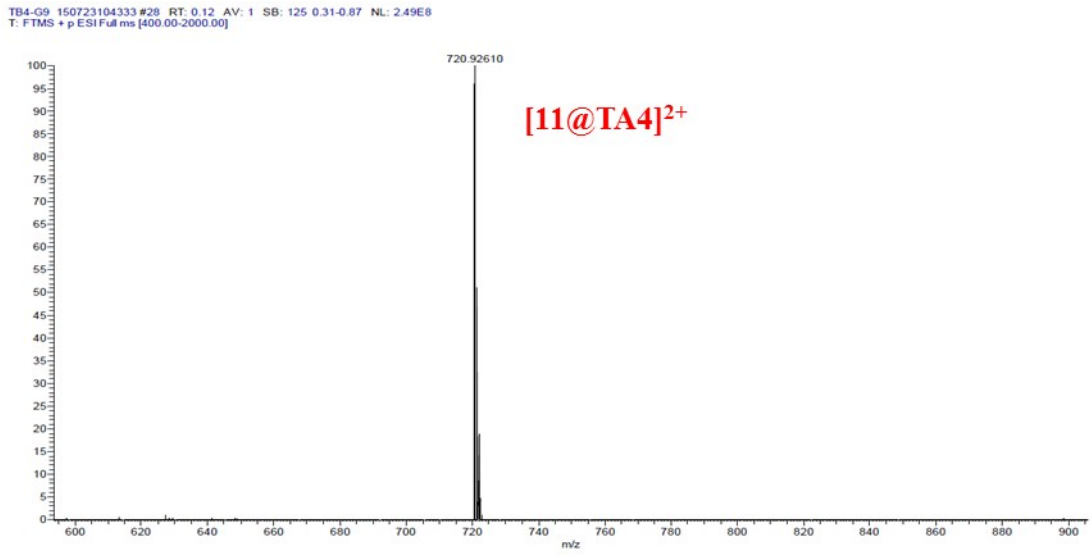

Fig. S23 ESI mass spectrum of **11-2PF$_6$@TA4**. The result indicates **11-2PF$_6$** and **TA4** form a 1:1 complex.

4. Binding Constants Determined by ITC

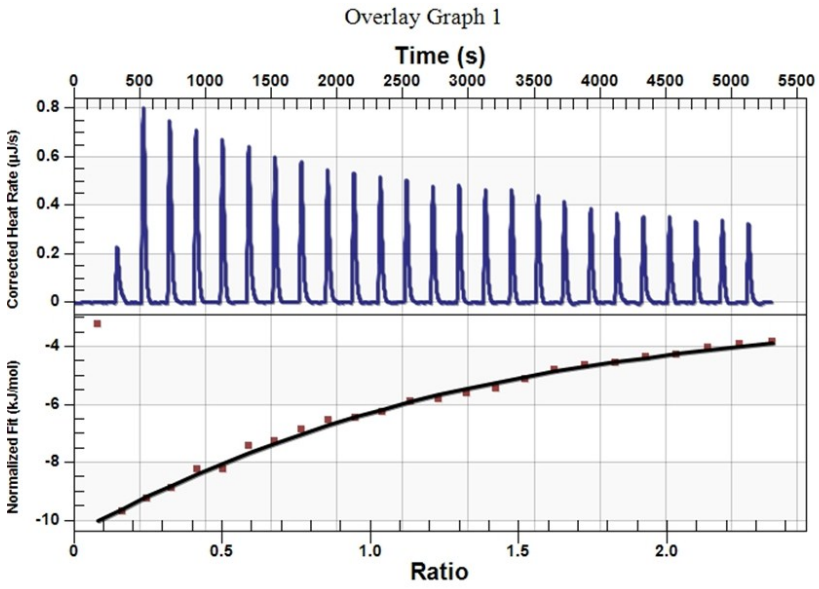

Fig. S24 Titration plots (heat flow versus time and heat versus guest/host ratio) obtained from ITC experiments of **TA4** with **1-PF_6** in the 1:1 mixture of 1,2-dichloroethane and CH_3CN.

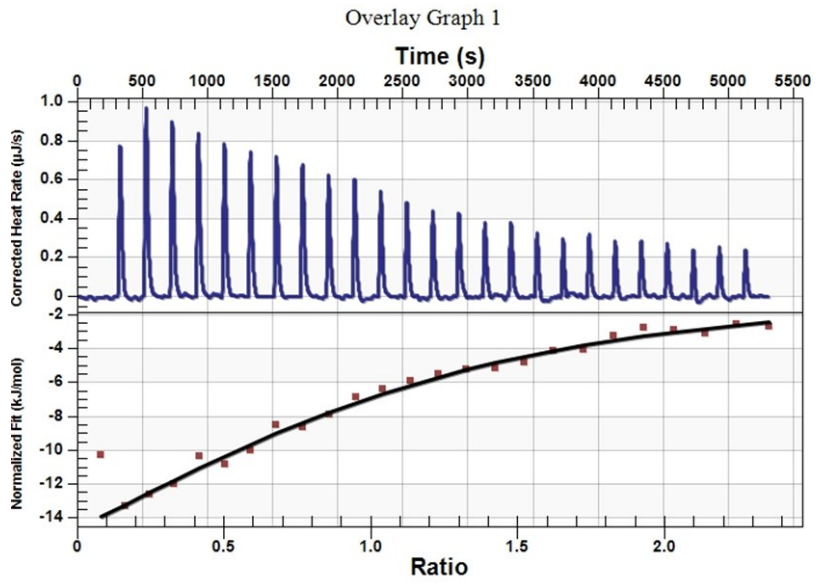

Fig. S25 Titration plots (heat flow versus time and heat versus guest/host ratio) obtained from ITC experiments of **TA4** with **2-PF_6** in the 1:1 mixture of 1,2-dichloroethane and CH_3CN.

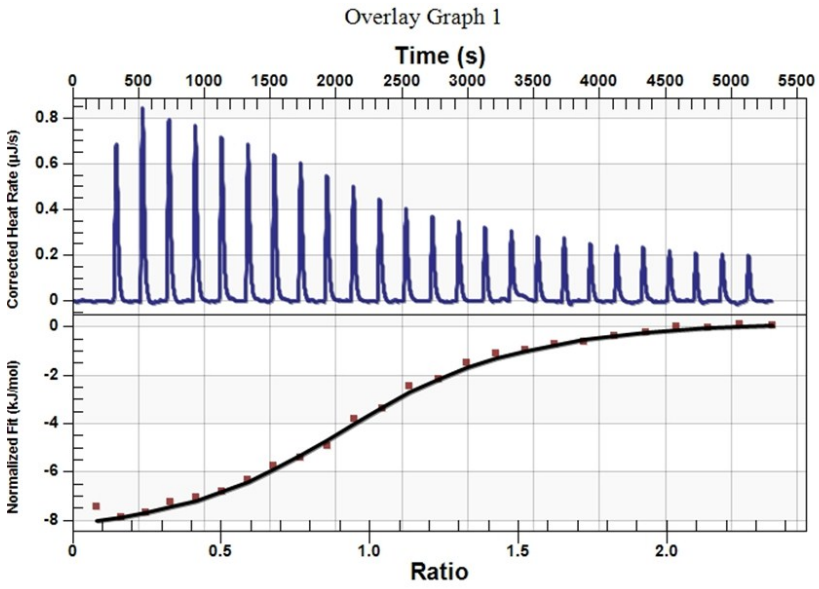

Fig. S26 Titration plots (heat flow versus time and heat versus guest/host ratio) obtained from ITC experiments of **TA4** with **5-PF_6** in the 1:1 mixture of 1,2-dichloroethane and CH_3CN.

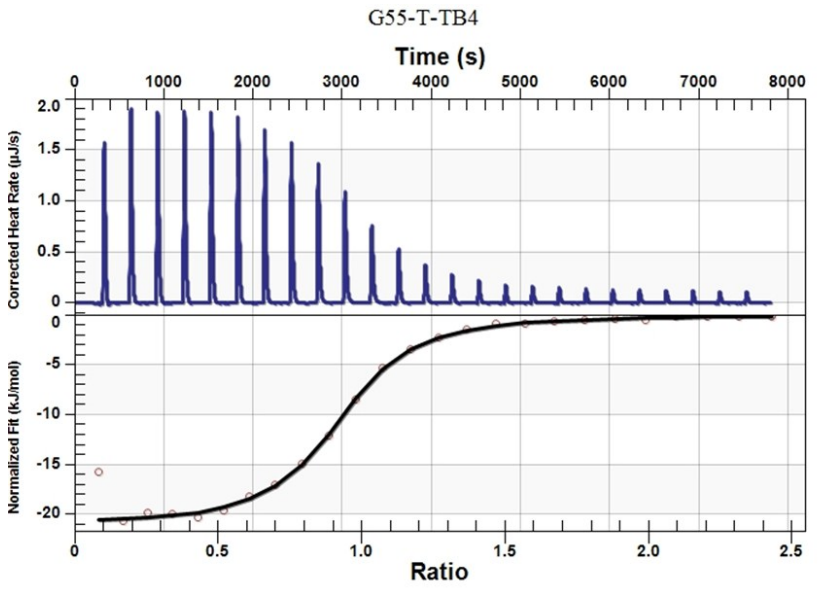

Fig. S27 Titration plots (heat flow versus time and heat versus guest/host ratio) obtained from ITC experiments of **TA4** with **6-PF_6** in the 1:1 mixture of 1,2-dichloroethane and CH_3CN.

5. Binding Constants Determined by Titration

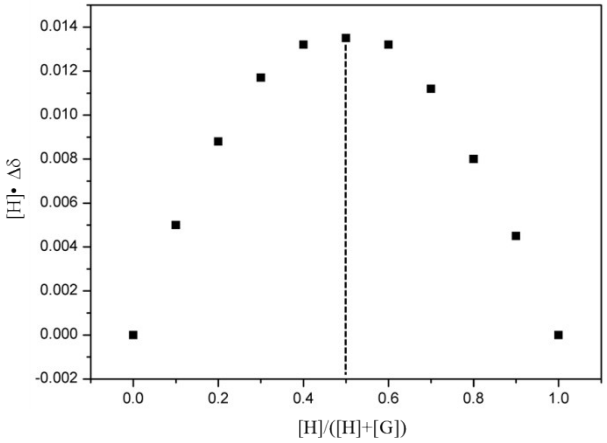

Fig. S28 Job's plot obtained by plotting the chemical shift change ($\Delta\delta$) of the Host's proton (a+b) in ^{1}H NMR spectra by varying the ratio of the host and the guest against the mole fraction of **TA4**. The total concentration of the host and the guest is fixed: [Host] + [Guest] = 2.0 mM. This experiment supports the 1:1 binding stoichiometry between **3-PF$_6$** and **TA4** in the 1:1 mixture of CD_2Cl_2 and CD_3CN.

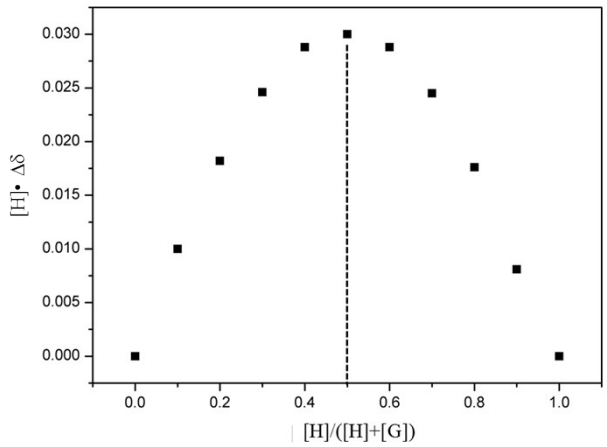

Fig. S29 Job's plot obtained by plotting the chemical shift change ($\Delta\delta$) of the Host's proton c in ^{1}H NMR spectra by varying the ratio of the host and the guest against the mole fraction of Host **TA4**. The total concentration of the host and the guest is fixed: [Host] + [Guest] = 2.0 mM. This experiment supports the 1:1 binding stoichiometry between **9-PF$_6$** and **TA4** in the 1:1 mixture of CD_2Cl_2 and CD_3CN.

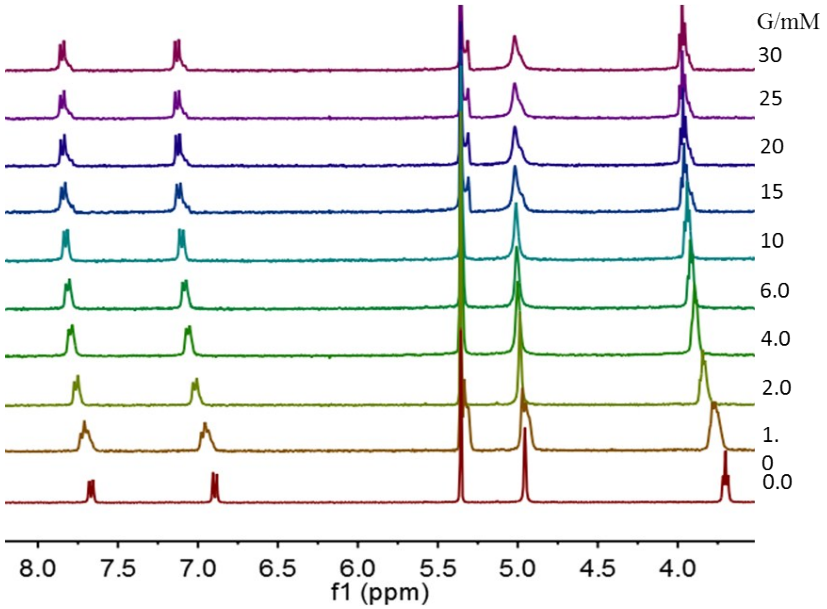

Fig. S30 Partial ^{1}H NMR spectra (400 MHz, CD_2Cl_2:CD_3CN=1:1, 298 K) of **TA4** (0.5 mM) titrated by **3-PF$_6$**. From bottom to top, the concentrations of **3-PF$_6$** are in the range of 0~30.0 mM. Protons (*a*+*b*) of **TA4** were monitored for the calculation of binding constants. This is the same for all the following experiments, unless otherwise noted. Nonlinear curve-fitting method[2] used here has been reported.

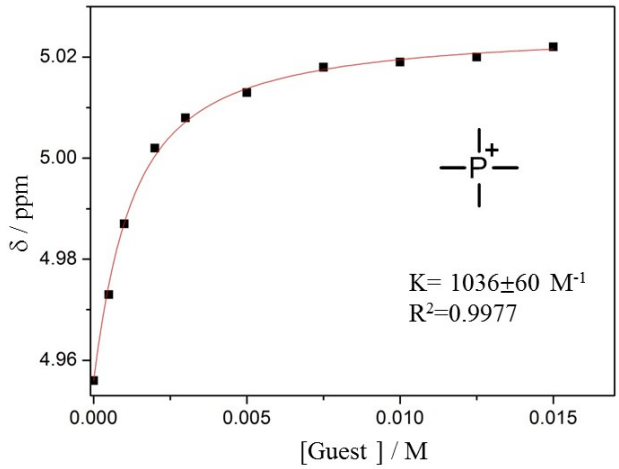

Fig. S31 Non-linear curve-fitting for the complexation between **TA4** and **3-PF$_6$** in the 1:1 mixture of CD_2Cl_2 and CD_3CN at 298 K.

2 G. Huang, Z. He, C.-X. Cai, F. Pan, D. Yang, K. Rissanen and W. Jiang. *Chem. Commun.* 2015, **51**, 15490-15493

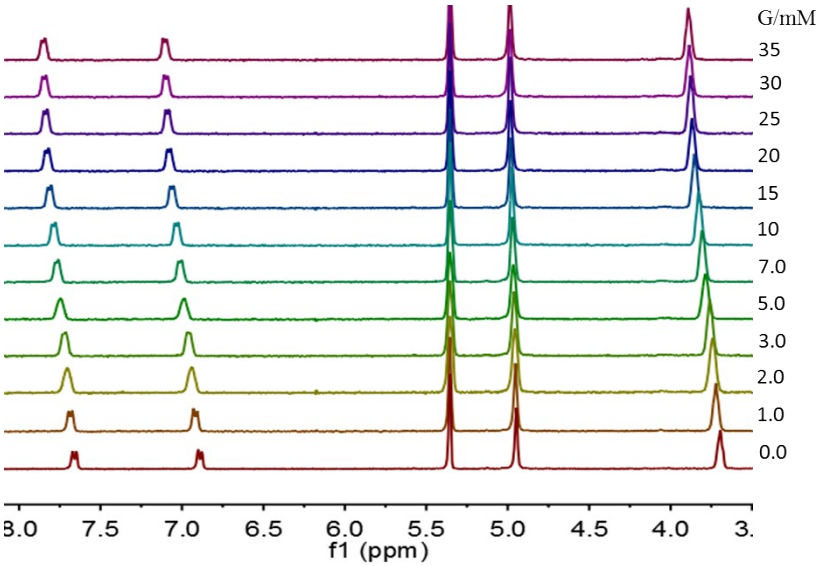

Fig. S32 Partial ^{1}H NMR spectra (400 MHz, CD_2Cl_2:CD_3CN=1:1, 298 K) of **TA4** (0.5 mM) titrated by **4-PF$_6$**. From bottom to top, the concentrations of **4-PF$_6$** are in the range of 0~35.0 mM.

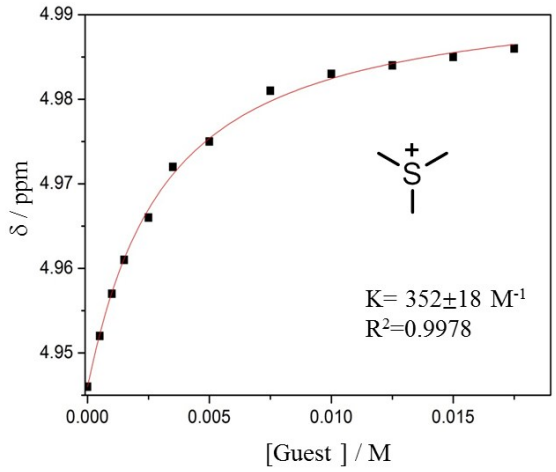

Fig. S33 Non-linear curve-fitting for the complexation between **TA4** and **4-PF$_6$** in the 1:1 mixture of CD_2Cl_2 and CD_3CN at 298 K.

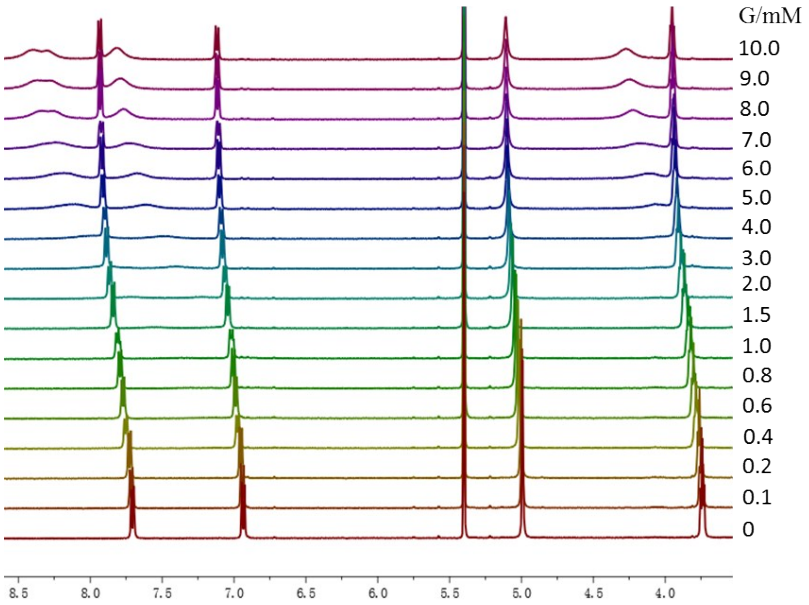

Fig. S34 Partial ^{1}H NMR spectra (400 MHz, CD_2Cl_2:CD_3CN=1:1, 298 K) of **TA4** (0.5 mM) titrated by **7-PF$_6$**. From bottom to top, the concentrations of **7-PF$_6$** are in the range of 0~10.0 mM.

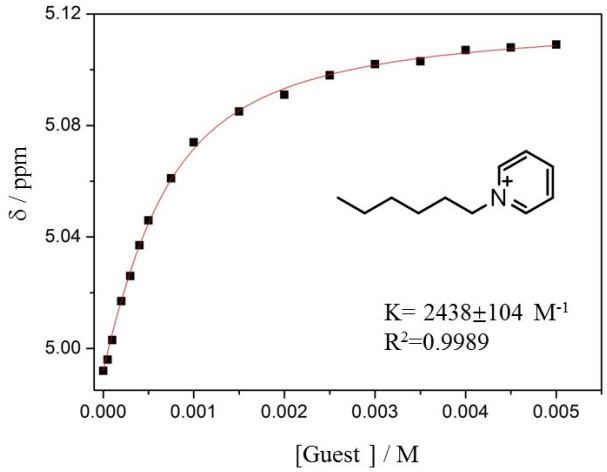

Fig. S35 Non-linear curve-fitting for the complexation between **TA4** and **7-PF$_6$** in the 1:1 mixture of CD_2Cl_2 and CD_3CN at 298 K.

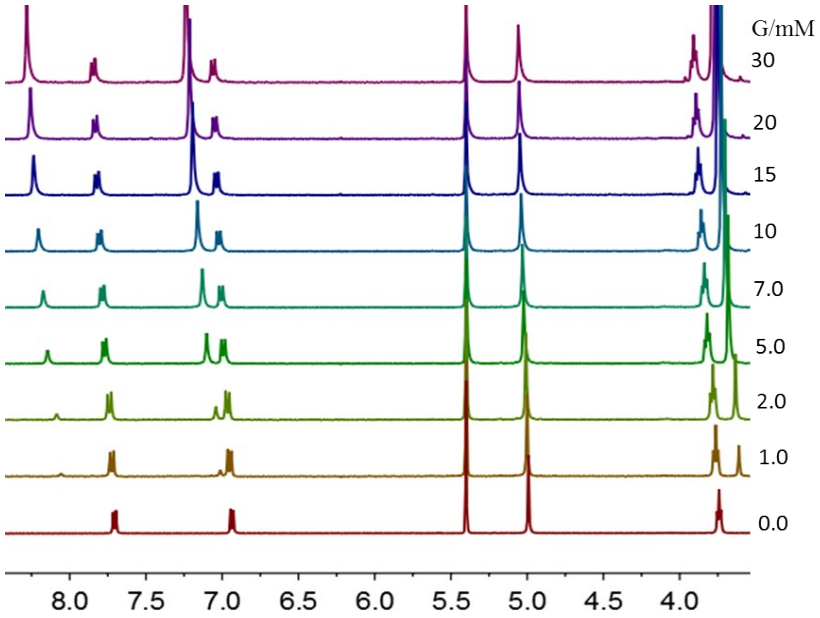

Fig. S36 Partial ^{1}H NMR spectra (400 MHz, CD_2Cl_2:CD_3CN=1:1, 298 K) of **TA4** (0.5 mM) titrated by **8-PF$_6$**. From bottom to top, the concentrations of **8-PF$_6$** are in the range of 0~30.0 mM.

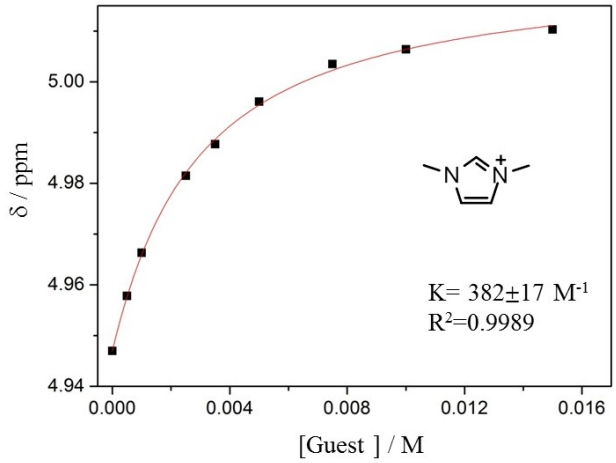

Fig. S37 Non-linear curve-fitting for the complexation between **TA4** and **8-PF$_6$** in the 1:1 mixture of CD_2Cl_2 and CD_3CN at 298 K.

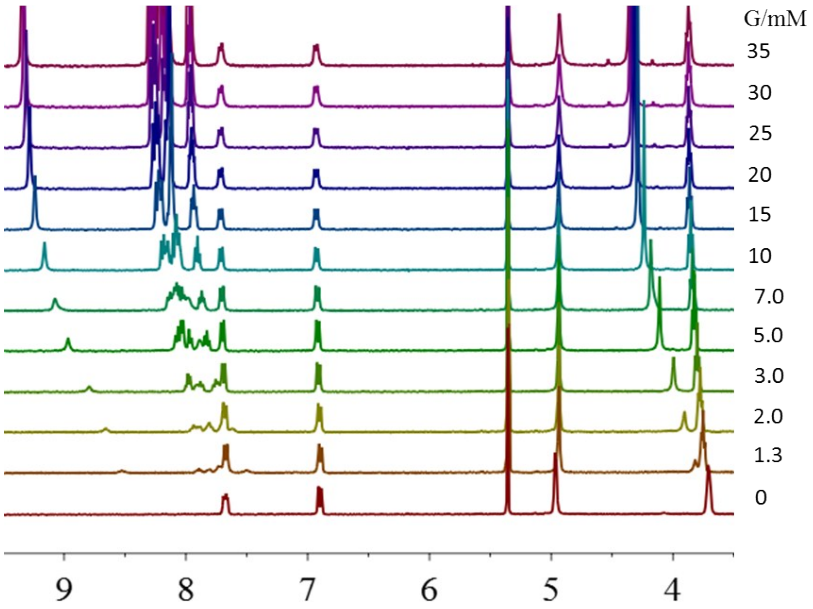

Fig. S38 Partial ^{1}H NMR spectra (400 MHz, CD_2Cl_2:CD_3CN=1:1, 298 K) of **TA4** (0.5 mM) titrated by **9-PF$_6$**. From bottom to top, the concentrations of **9-PF$_6$** are in the range of 0~35.0 mM. The chemical shifts of proton *c* of **TA4** were monitored for the calculation of binding constants.

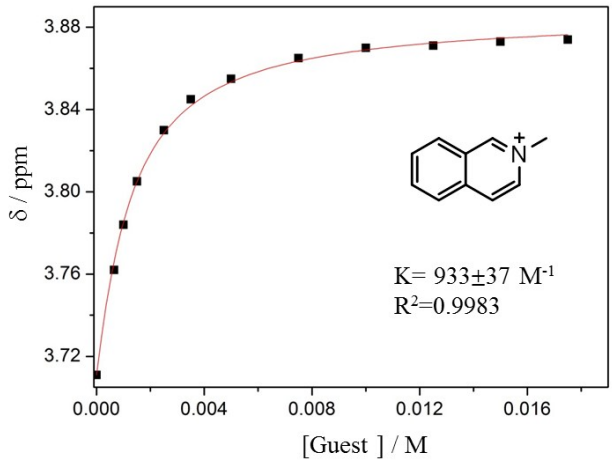

Fig. S39 Non-linear curve-fitting for the complexation between **TA4** and **9-PF$_6$** in the 1:1 mixture of CD_2Cl_2 and CD_3CN at 298 K.

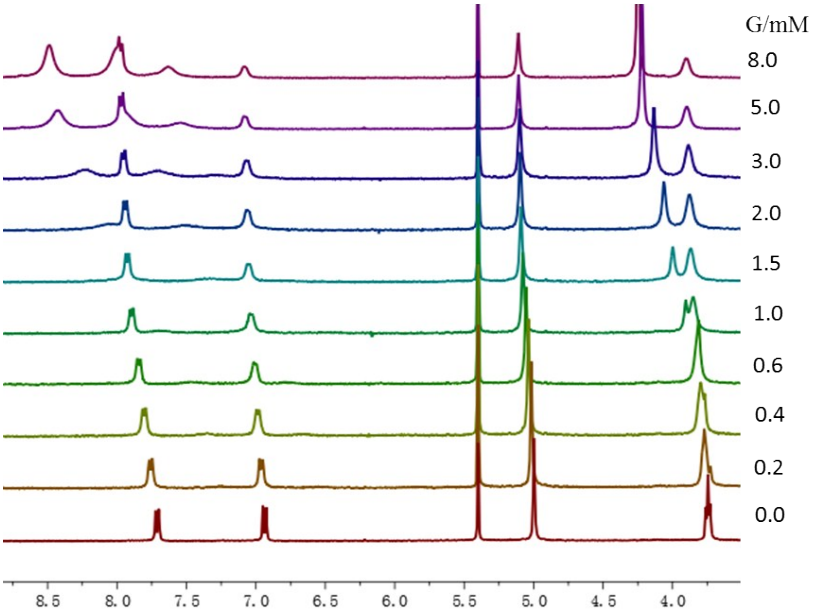

Fig. S40 Partial ^{1}H NMR spectra (400 MHz, CD_2Cl_2:CD_3CN=1:1, 298 K) of **TA4** (0.5 mM) titrated by **10-2PF$_6$**. From bottom to top, the concentrations of **10-2PF$_6$** are in the range of 0~8.0 mM.

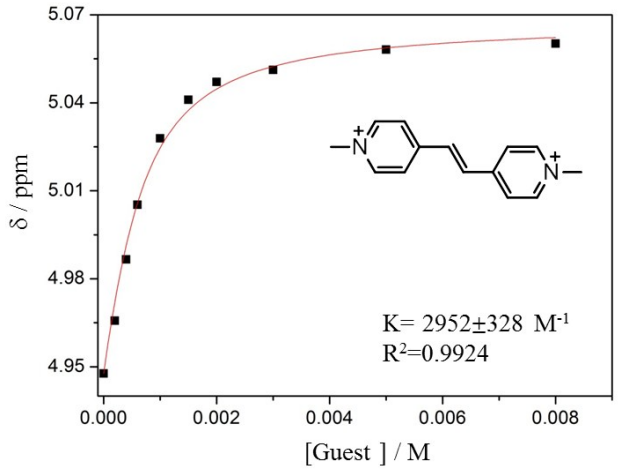

Fig. S41 Non-linear curve-fitting for the complexation between **TA4** and **10-2PF$_6$** in the 1:1 mixture of CD_2Cl_2 and CD_3CN at 298 K.

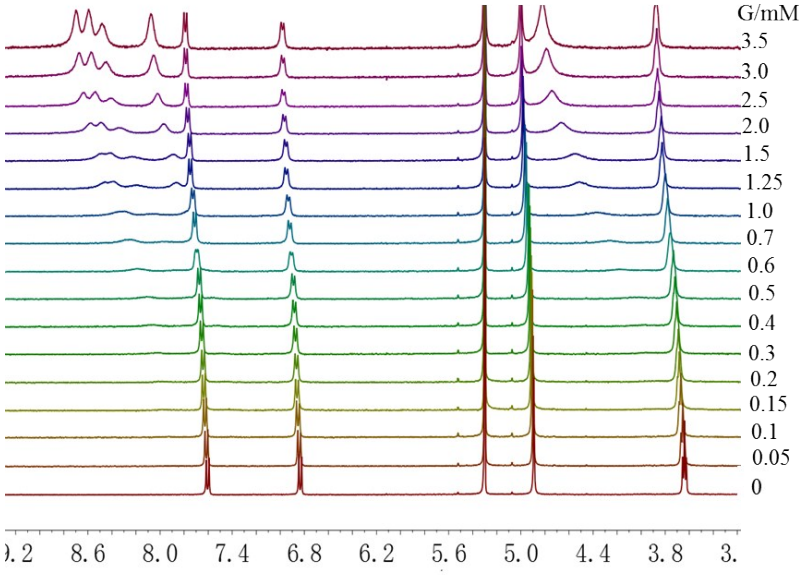

Fig. S42 Partial ^{1}H NMR spectra (400 MHz, CD_2Cl_2:CD_3CN=1:1, 298 K) of **TA4** (0.5 mM) titrated by **11-2PF$_6$**. From bottom to top, the concentrations of **11-2PF$_6$** are in the range of 0~3.5 mM.

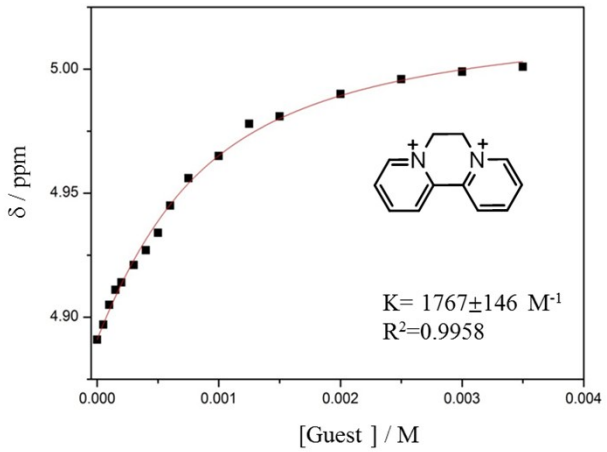

Fig. S43 Non-linear curve-fitting for the complexation between **TA4** and **11-2PF$_6$** in the 1:1 mixture of CD_2Cl_2 and CD_3CN at 298 K.

6. Solvent-Dependent NMR Spectra

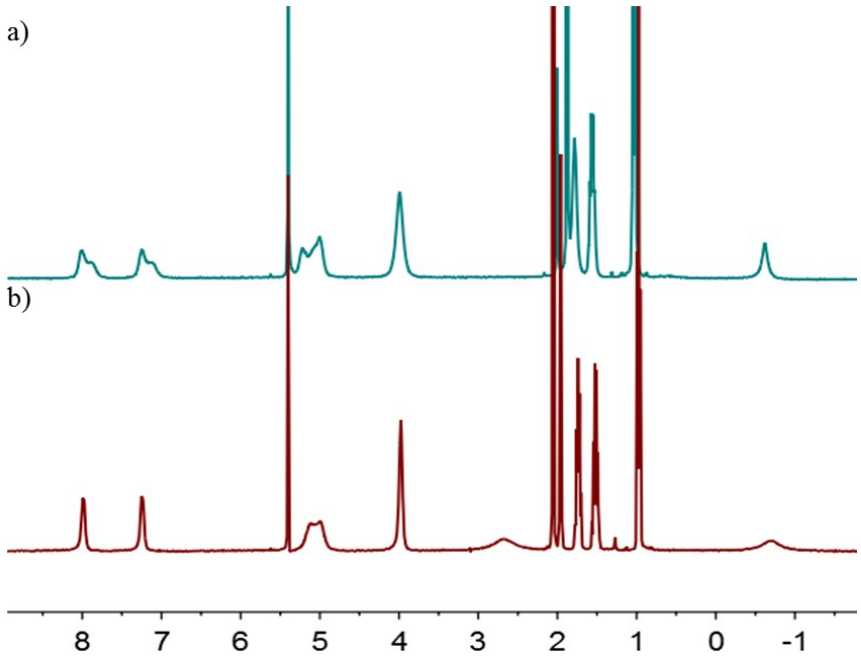

Fig. S44 ^{1}H NMR spectra (400 MHz, 2.0 mM, 298 K) of the equimolar mixture of **1-PF_6@TA4** in the (a) 5:1 or (b) 1:1 mixture of CD_2Cl_2 and CD_3CN.

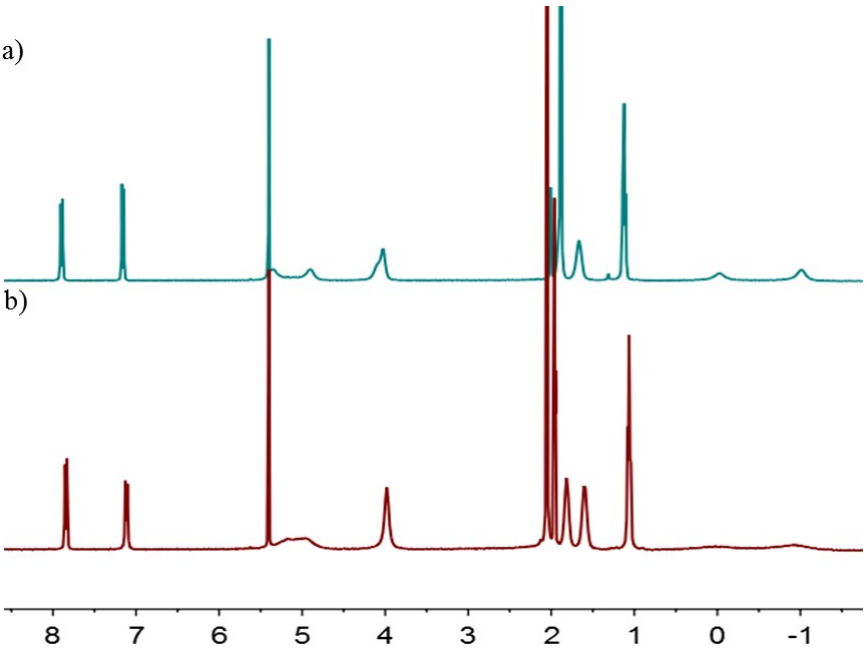

Fig. S45 ^{1}H NMR spectra (400 MHz, 2.0 mM, 298 K) of the equimolar mixture of **2-PF_6@TA4** in the (a) 5:1 or (b) 1:1 mixture of CD_2Cl_2 and CD_3CN.

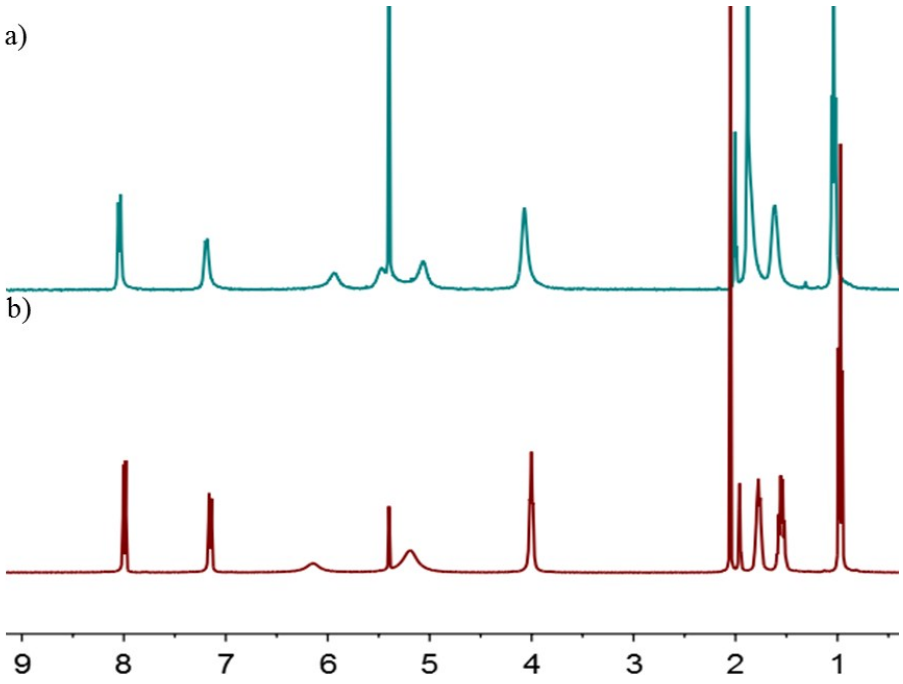

Fig. S46 ^{1}H NMR spectra (400 MHz, 2.0 mM, 298 K) of the equimolar mixture of **5-PF$_6$@TA4** in the (a) 5:1 or (b) 1:1 mixture of CD_2Cl_2 and CD_3CN.

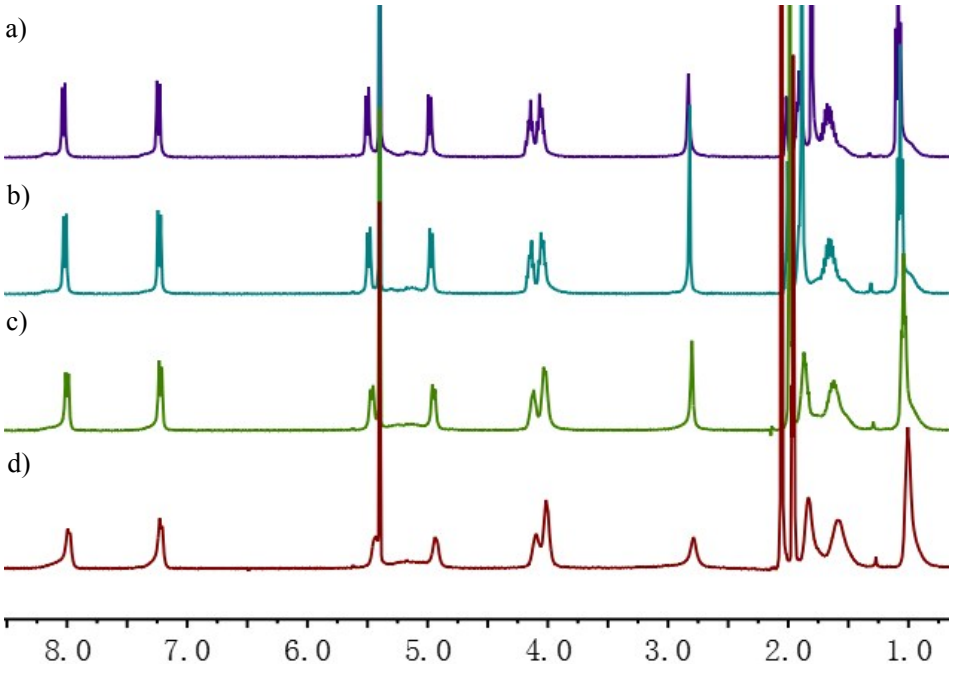

Fig. S47 ^{1}H NMR spectra (400 MHz, 2.0 mM, 298 K) of the equimolar mixture of **6-PF$_6$@TA4** in the (a) 10:1, (b) 5:1, (c) 2:1 or (d) 1:1 mixture of CD_2Cl_2 and CD_3CN.

7. 2D NMR Spectra of the Complexes

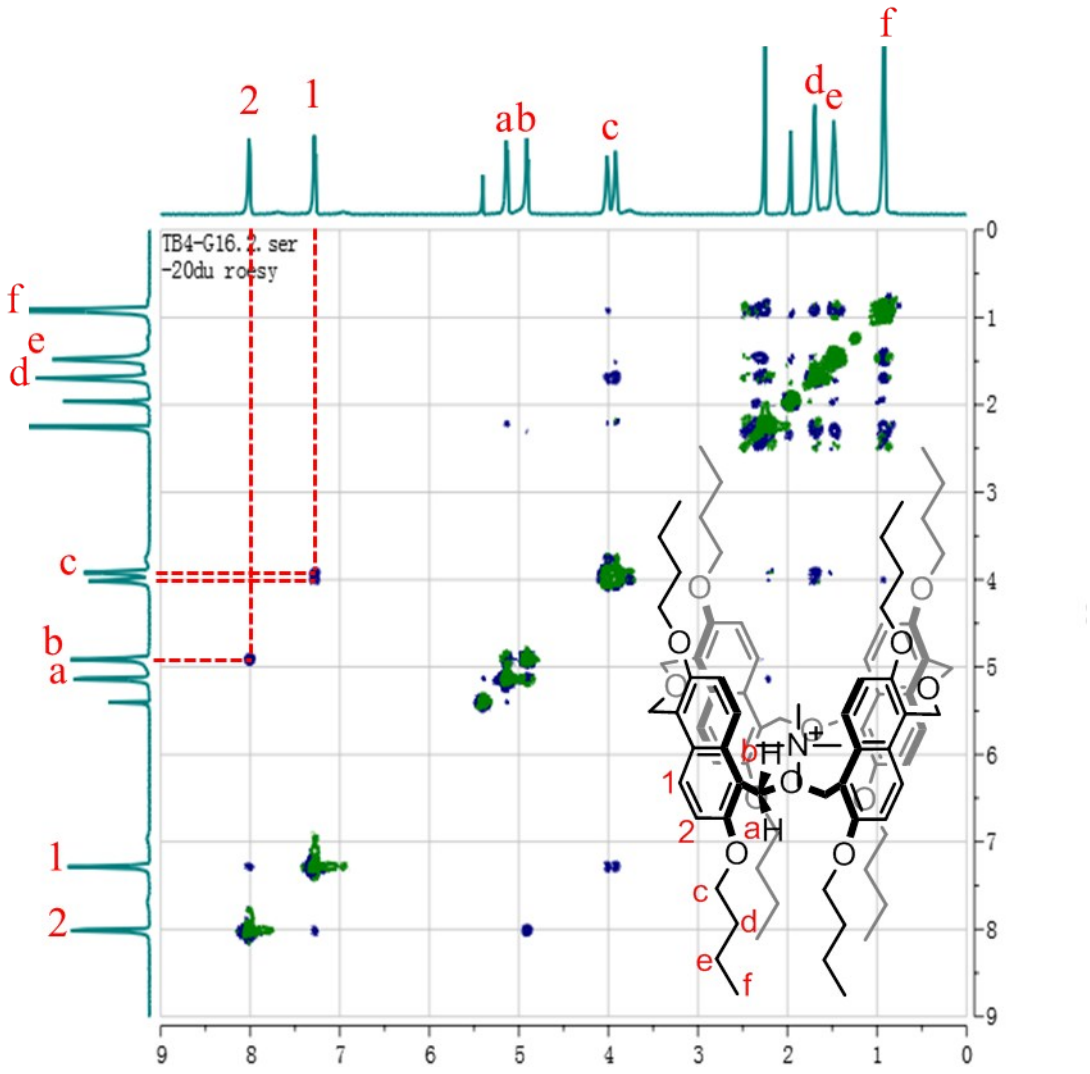

Fig. S48 ^{1}H,^{1}H-ROESY NMR spectra (600 MHz, CD_2Cl_2:CD_3CN=1:1, 6.0 mM,) of **1-PF$_6$@TA4** at -20°C. This result supports that **TA4** in this complex predominantly exists as conformation **I**.

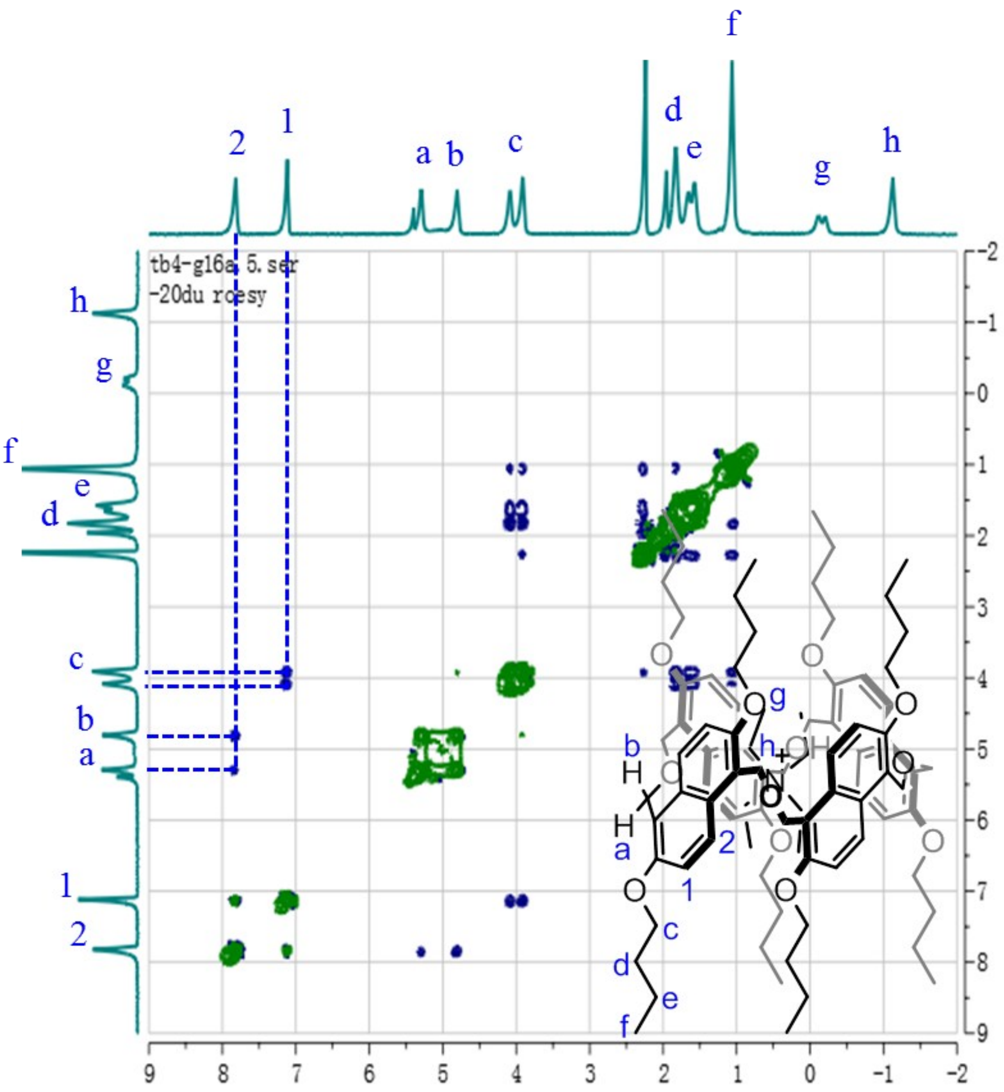

Fig. S49 ^{1}H,^{1}H-ROESY NMR spectra (600 MHz, CD_2Cl_2:CD_3CN=1:1, 6.0 mM,) of **2-PF$_6$@TA4** at -20^{o}C. This result supports that **TA4** in this complex predominantly exists as conformation **IV**.

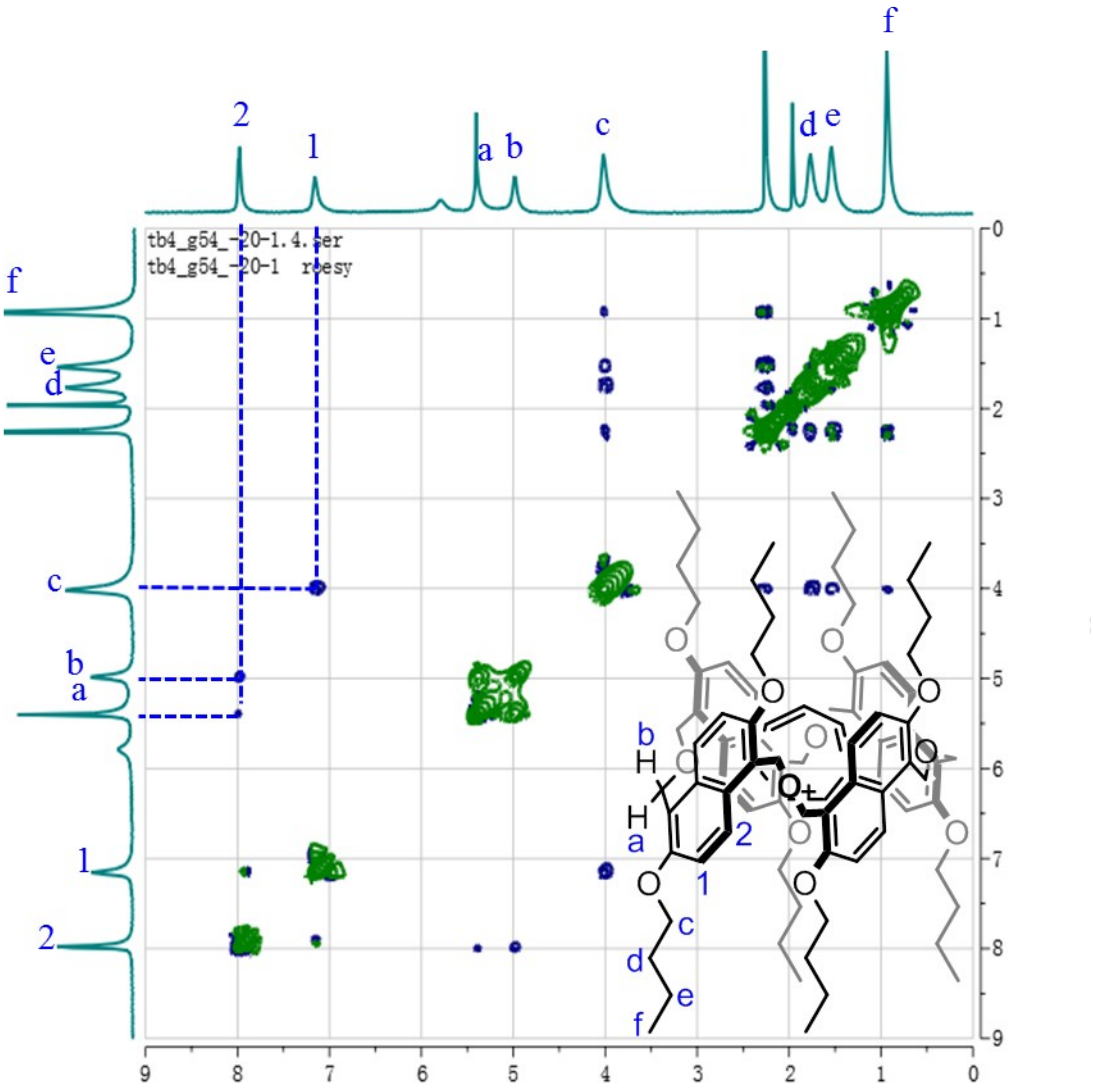

Fig. S50 ^{1}H,^{1}H-ROESY NMR spectra (600 MHz, CD_2Cl_2:CD_3CN=1:1, 6.0 mM,) of **5-PF_6@TA4** at -20°C. This result supports that **TA4** in this complex predominantly exists as conformation **IV**.

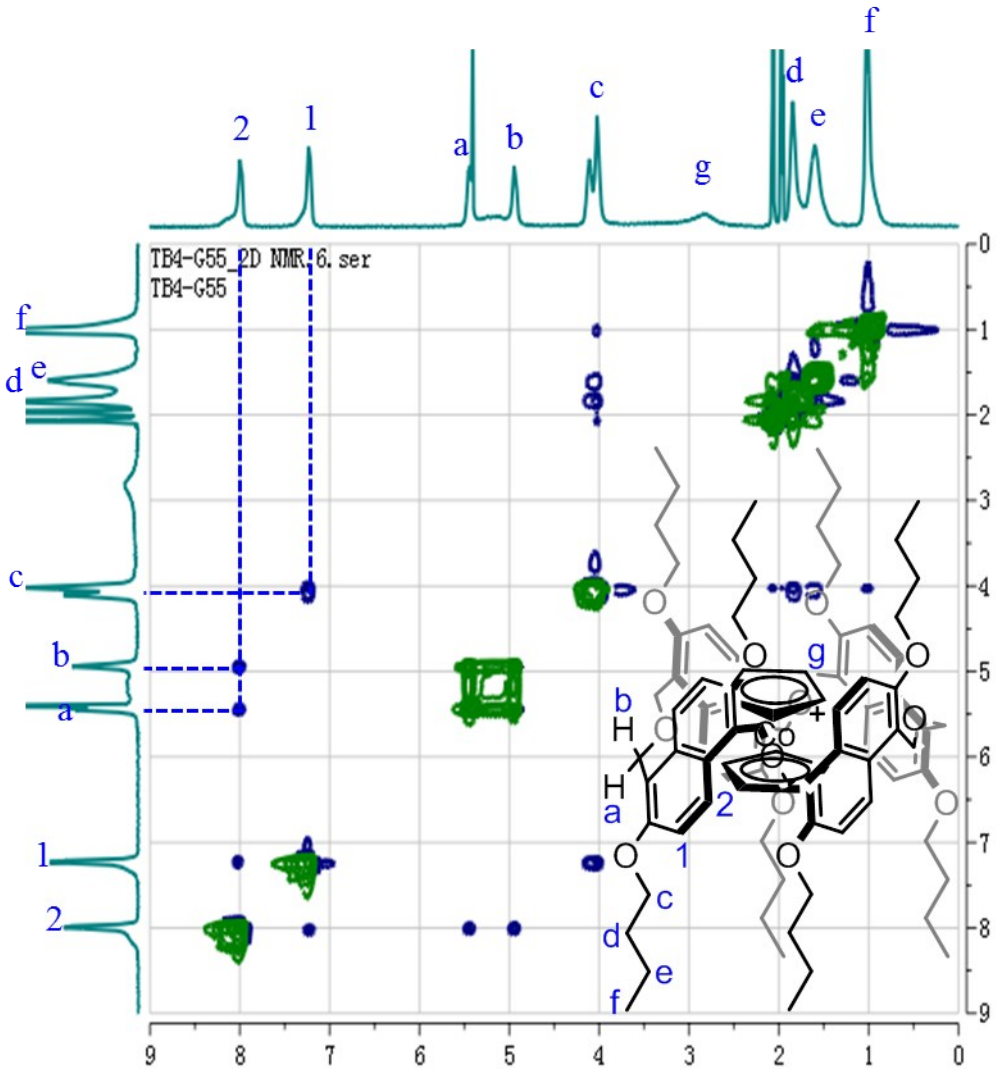

Fig. S51 ^{1}H,^{1}H-ROESY NMR spectra (600 MHz, CD_2Cl_2:CD_3CN=1:1, 6.0 mM,) of **6-PF_6@TA4** at -20°C. This result supports that **TA4** in this complex predominantly exists as conformation **IV**.